Records of past mid-depth ventilation: Cretaceous Ocean Anoxic Event 2 *vs*. Quaternary Oxygen Minimum Zones

J. Schönfeld[1], W. Kuhnt[2], Z. Erdem[1], S. Flögel[1], N. Glock[1], M. Aquit[2], M. Frank[1] and A. Holbourn[2]

[1]{GEOMAR Helmholtz Centre for Ocean Research, Kiel, Germany }

[2]{Institute for Geosciences, Christian-Albrechts-University, Kiel, Germany }

Correspondence to: J. Schönfeld (jschoenfeld@geomar.de)

Abstract

Present day oceans are well ventilated except mid-depth oxygen minimum zones (OMZs) under high surface water productivity, regions of sluggish circulation, and restricted marginal basins. In the Mesozoic, however, entire oceanic basins transiently became dysoxic or anoxic. The Cretaceous Ocean Anoxic Events (OAEs) were characterised by laminated organic-carbon rich shales and low-oxygen indicating trace fossils preserved in the sedimentary record. Yet assessments of the intensity and extent of Cretaceous near-bottom water oxygenation have been hampered by deep or long-term diagenesis and the evolution of marine biota serving as oxygen indicators in today's ocean. Sedimentary features similar to those found in Cretaceous strata were observed in deposits underlying Recent OMZs, where bottom-water oxygen levels, the flux of organic matter, and benthic life are well studied. Their implications for constraining past bottom-water oxygenation are addressed in this review. We compared OMZ sediments from the Peruvian upwelling with deposits of the late Cenomanian OAE 2 from the NW African shelf. Holocene laminated sediments are encountered at bottom-water oxygen levels of <7 μmol kg^{-1} under the Peruvian upwelling and <5 μmol kg^{-1} in California Borderland basins and the Pakistan Margin. Seasonal to decadal changes of sediment input are necessary to create laminae of different composition. However, bottom currents may shape similar textures that are difficult to discern from primary seasonal laminae. The millimetre-sized trace fossil *Chondrites* was commonly found in Cretaceous strata and Recent oxygen-depleted environments where its diameter increased with oxygen

levels from 5 to 45 μmol kg^{-1}. *Chondrites* has not been reported from Peruvian sediments but cm-sized crab burrows appeared around 10 μmol kg^{-1}, which may indicate a minimum oxygen value for bioturbated Cretaceous strata. Organic carbon accumulation rates ranged from 0.7 and 2.8 g C cm^{-2} kyr^{-1} in laminated OAE 2 sections in Tarfaya Basin, Morocco, matching late Holocene accumulation rates of laminated Peruvian sediments under Recent oxygen levels below 5 μmol kg^{-1}. Sediments deposited at >10 μmol kg^{-1} showed an inverse exponential relationship of bottom-water oxygen levels and organic carbon accumulation depicting enhanced bioirrigation and decomposition of organic matter with increased oxygen supply. In absence of seasonal laminations and under conditions of low burial diagenesis, this relationship may facilitate quantitative estimates of paleo-oxygenation. Similarities and differences between Cretaceous OAEs and late Quaternary OMZs have to be further explored to improve our understanding of sedimentary systems under hypoxic conditions.

1 Introduction

In the present day ocean, most of the water column is well ventilated as a consequence of thermohaline circulation processes that lead to subduction of cold, oxygen rich and dense water masses in high northern and southern latitudes (e.g. Kuhlbrodt et al., 2007). Exceptions are restricted basins, in which the limited exchange with the oxygen rich water masses of the open ocean is not sufficient to counteract oxygen consumption by organic matter respiration such as in the Black Sea (Murray et al., 1989). In the open ocean, strongly oxygen depleted water bodies occur underlying highly productive surface waters such as in the major upwelling areas off the western continental margins of Africa and the Americas or below the monsoon-driven upwelling of the Arabian Sea (Helly and Levin, 2004). In the geological past, regional or global ventilation of the ocean underwent significant changes on different time scales due to a variety of reasons, including changes in atmospheric and ocean circulation, stratification, temperature or tectonic processes. It is, however, difficult to quantify the past spatial extent and intensity of oxygen minima because the oxygen concentration of the water column is not directly recorded in the sediments. As a consequence, derivative proxies have been applied to reconstruct past ocean oxygenation.

A characteristic feature of marine low-oxygen environments on various time scales are black, organic-rich, and laminated sediments (Kemp, 1996; Meyer and Kump, 2008). They are known since the late Precambrian (Tucker, 1983). Widespread and contemporaneous

occurrences of these deposits in Devonian, Permian, early Jurassic, early and late Cretaceous, and mid-Miocene successions depict periods of sluggish ocean circulation or extensive highly productive seas (Schlanger and Jenkyns, 1976; Buggisch, 1991; Flower and Kennett, 1993; Wignall and Twitchett, 1996; Trabucho-Alexandre et al., 2010). The question whether these laminated sediments were formed due to enhanced primary production or due to restricted ventilation of near-bottom waters has fueled a long-lasting debate (e.g. Calvert, 1987). Yet the discovery of laminated sediments in the Arabian Sea during the International Indian Ocean Expedition in 1965 revealed that this sedimentary facies is confined to OMZs at mid-depth (Schott et al., 1970). Laminated sediments at the southwest African, Peruvian and Californian margin provided further evidence for their association with today's OMZs (van Andel, 1964; Reimers and Suess, 1983; Struck et al., 2002;). In contrast, basinwide stagnation events resulting in the deposition of organic-rich, at least partially laminated sediments were recorded during short time intervals with specific environmental settings from the Pliocene to early Holocene in the eastern Mediterranean (sapropels) and in the Sea of Japan (Stein and Stax, 1990; Rohling and Hilgen, 1991). They are, however, not considered potential analogues for the extensively occurring black, laminated shales of the Mesozoic including the Cretaceous OAEs (Erbacher et al., 2001).

Stable carbon isotope data obtained from Devonian, Toarcian, Aptian and Cenomanian/Turonian successions revealed that the organic-rich beds recorded profound perturbations of the global biogeochemical cycles, of which the Cenomanian/Turonian boundary interval (OAE2) was probably the most extensive event (e.g. Jenkyns et al., 1994; Hesselbo et al., 2000; Joachimski et al., 2002; Herrle et al., 2004). Detailed investigations of the geochemistry, microfossil assemblages, and sedimentary structures of both, recent and fossil strata were performed to unravel the interplay of local, regional and global processes driving their formation, and to enforce a mutual understanding of late Quaternary OMZs and Cretaceous OAEs (Thiede and Suess, 1983; Anbar and Rouxel, 2007; Dale et al., 2012; Owens et al., 2013). These studies were complemented by oceanographic, biological and biochemical studies in recent upwelling systems and OMZs. However, this actualistic approach has been hampered by long periods of burial, diagenesis, and evolution of the biosphere since their deposition in Mesozoic times.

Geochemical redox proxies were extensively explored on Cretaceous black shales in order to constrain past ocean oxygenation, in particular trace metals (Brumsack, 2006;

van Bentum et al., 2009; Dale et al., 2012), sulfur isotopes (Hetzel et al., 2009; Owens et al., 2013), and iron isotopes (Owens et al., 2012). Some of these proxies have also been measured on surface sediments and sediment cores from the Peruvian OMZ, in particular U/Mo ratios (Böning et al., 2004, Scholz et al., 2011, 2014a, b). However, only a very few data points are available for a regional U/Mo – bottom-water oxygen calibration in the Peruvian OMZ (Scholz et al., 2011). They strongly differ from corresponding data obtained from other OMZs (McManus et al., 2006). This hampers a quantititative reconstruction of past oxygenation with U/Mo ratios for the Peruvian OMZ as well as for black shales from Cretaceous of OAE2.

Besides geochemical redox indicators, there are only few other reliable parameters that are sufficiently explored to investigate paleo low-oxygen conditions in the Mesozoic and Cenozoic, which are trace fossils, laminations, and organic carbon accumulation rates. Their potential, constraints, and implications for an assessment of past water column oxygenation are addressed in this review. Particular emphasis is put on the comparison of Holocene OMZ sediments from the upwelling area off Peru with deposits of Cretaceous Oceanic Anoxic Event 2 from the Moroccan shelf.

2 Material and Methods

The Peruvian Margin study is based on stratigraphic and sedimentological data from 136 sediment cores within and below today's OMZ off the western South American continental margin. They are located between the Equator and 18°S and were retrieved from water depths between 180 and 2200 m (Figure 1). Data of 94 cores were taken from the literature and 42 new cores recovered during R/V METEOR cruises M77/1 and M77/2 in 2008 were assessed as part of this study (Appendix Table A1). The cruises were performed in the framework of Collaborative Research Centre (SFB) 754 "Climate Biogeochemistry Interactions in the Tropical Ocean", through which supplementary data for the environmental interpretation of the sedimentary records are available.

In particular, oxygen concentrations along the Peruvian continental margin were measured during R/V METEOR cruises M77-1, M77-2 (Krahmann, 2012) and M77-3 (Kalvelage et al., 2013). We considered 159 CTD stations with a maximum water depth of 1750 m and a maximum distance of 175 km to the shore (online supplement M77-1-3_CTD_Data.xls). Other CTD casts further offshore were not included because they already showed significantly elevated oxygen concentrations compared to proximal locations at the same

latitude. Kalvelage et al. (2013) observed an offset of ~2 µmol/kg between the CTD attached optode oxygen sensors and the more sensitive STOX sensors, which are based on a Clark-type oxygen sensor, and corrected the optode data by 2 µmol/kg during the cruises M77-3 and M77-4. The oxygen data presented in our study were not corrected for a 2 µmol/kg offset since the STOX sensors were not deployed during M77-1 and M77-2.

We considered visual core descriptions, physical property data, in particular dry bulk densities, sand content and abundances of biogenic, terrigenous and diagenetic components, and organic carbon contents. The chronostratigraphy of the cores was established with radiocarbon datings on monospecific samples of planktonic or benthic foraminifera, or bulk sedimentary organic carbon.

The age models of the cores from M77/1 and M77/2 cruises are based on Mollier-Vogel et al. (2013). Otherwise, published, conventional radiocarbon ages and new ^{14}C Accelerator Mass Spectrometer (AMS) datings were calibrated using the software "Calib 7.0" (Stuiver and Reimer, 1993) and by applying the marine calibration set "*Marine13"* (Reimer et al., 2013). Reservoir age corrections (ΔR) were carried out by using the Marine Reservoir Correction Database (http://calib.qub.ac.uk/marine/). Regionally weighted mean ΔR values rangedfrom 89 to 338 years for the eastern Pacific off Peru. The uncertainties of the source data ranged from ±31 to ±82 years (2-sigma). For the pre-Holocene part of the records, the radiocarbon-based chronologies were supplemented with planktonic and benthic oxygen isotope curves correlated to stacked reference records (e.g. Liesicki and Raymo, 2005) or Antarctic ice cores (e.g. EPICA Community Members, 2006). Subrecent sedimentation rates were constrained by ^{210}Pb excess activity profiles (Reimers and Suess, 1983; Mosch et al., 2012). All ages are given in calendar years before 1950 AD (abbreviated as cal. ka.). Organic carbon and bulk sediment accumulation rates (g cm^{-2} kyr^{-1}) were calculated from linear sedimentation rates (cm 10^{-3} years) and bulk dry densities (g cm^{-3}) following van Andel et al. (1975).

The M77/1 and M77/2 cores included in this study were described immediately after opening aboard R/V METEOR (Pfannkuche et al., 2011). Two parallel series of volume-defined samples were taken in 5 or 10-cm intervals with cut-off syringes. One series of 10-cc samples was freeze-dried and physical properties were determined from wet sample volumes and the weight loss after drying applying standard protocols and a pore-water density of 1.026 g cm^{-3} (Boyce, 1976). The other series of 20-cc samples dedicated to isotopic measurements,

microfossil, and sand-fraction examination was washed gently with tap water through a 63 µm sieve within a few hours after sampling. Washing of fresh, wet samples facilitates a better preservation of delicate calcareous microfossils, which otherwise may have been corroded or even dissolved by oxidation products of ferrosulphides and labile organic matter (Schnitker et al., 1980). The residues were dried at 50°C and weighed. For stable oxygen and carbon isotope analyses, about 30 specimens of the planktonic foraminiferal species *Globigerinoides ruber* (white), *Neogloboquadrina dutertrei* or 3 to 6 specimens of the benthic species *Uvigerina striata*, *U. peregrina* or *Globobulimina pacifica* were picked from the size fractions 250 to 355 µm or >63 µm, respectively. We used these species because they were abundant in the cores studied and incorporate stable oxygen isotopes in equilibrium with the surrounding pore and supernatant bottom waters (e.g. McCorkle et al., 1990). Oxygen and carbon isotopes were measured with a Thermo Fisher Scientific 253 Mass Spectrometer coupled to a CARBO KIEL automated carbonate preparation device at GEOMAR, Kiel. The long-term analytical precision (1-sigma) for $\delta^{18}O$ and $\delta^{13}C$ was better than 0.06 ‰ and 0.03 ‰ on the VPDB scale, respectively, based on more than 1000 measurements of an in-house carbonate standard during the respective measurement sessions. Replicate measurements of benthic foraminifera from the same sample showed an external reproducibility of ±0.1 ‰ for $\delta^{18}O$. For radiocarbon analyses, 33 to 179 specimens of *Planulina limbata* or 229 to 250 specimens of *Neogloboquadrina dutertrei* were picked from the size fraction >63 µm or 5 to 20 mg of ground bulk sediment was prepared. AMS measurements were performed at the Leibniz Laboratory for Radiometric Dating and Stable Isotope Research, University of Kiel (CAU) and at Beta Analytic Inc. Dried samples used for physical properties measurements were ground with an agate mortar. Aliquot subsamples of 3 to 20 mg were analysed for total carbon and organic carbon content with a Carbon Erba Element Analyzer (NA1500) at GEOMAR, Kiel. The long-term precision was ±0.6 % of the measured values as revealed by repeated measurements of two internal carbon standards.

Since the pioneering work of Einsele and Wiedmann (1975), Cenomanian to Lower Campanian organic-rich marlstones of the Tarfaya Basin in southern Morocco have been studied as a type locality of Cretaceous upwelling-related sediments at the eastern margin of the central North Atlantic (Wiedmann et al., 1978; Leine et al., 1986; Kuhnt et al., 1997, 2001, 2005; Kolonic et al., 2005; Aquit et al., 2013). Numerical climate and circulation models of the mid-Cretaceous Atlantic support a prevalence of cool and nutrient-rich intermediate deep water masses in this area along the NW African margin (Poulsen et al.,

2001; Topper et al., 2011). The late Cenomanian to early Turonian OAE 2 sediments discussed here were examined in outcrop sections during five field expeditions of the Kiel Micropaleontology Group in 1997, 1998, 2000, 2003 and 2009. In addition, core material from two commercial wells (S13 and S75), and a 350 m deep research well drilled in October-December 2009 (Tarfaya SN°4) were considered in this study (Figure 1).

Analytical methods applied to samples from outcrops and drill cores were detailed in Kuhnt et al. (2005) and Aquit et al. (2013). Core sections from the new exploration well Tarfaya SN°4 were cut lengthwise and described. Line scan measurements and photographs were acquired with a Ja CVL 1073 CCD color line scan camera with 3 sensors of 2048 pixels and Dichroic RGB beam splitter prism (RGB channels at 630 nm, 535 nm and 450 nm) at the Institute of Geosciences, Kiel University. Color measurement in L*a*b* units are from RGB digital images. Scanning was performed (resolution of 143 pixel per 70 micron) on the polished surface of oriented cores. Intensity of lamination vs. bioturbational homogenization of the sediment was estimated using high resolution lightness (L*) measurements for cores of SN°4. We calculated a lamination index based on a moving window standard deviation of the lightness values, similar to the method previously applied on core S75 (Kuhnt et al., 2005). Organic carbon and carbonate contents of SN°4 core samples were measured with a Carbon Erba Element Analyzer (NA1500) at Geomar, and with a conventional carbonate bomb at the Institute of Geosciences, Kiel University.

3 Results

3.1 Holocene to Recent organic-rich sedimentation underneath Recent OMZs

Bioturbation

Organisms dwelling in sediments below the redox boundary commonly rely on oxygen supply from the above near-bottom waters (Savrdaand Bottjer, 1991). They disappear if bottom-water oxygenation drops below a certain limit (Rhoads and Morse, 1971; Savrdaet al., 1984). Observations from Recent OMZs suggested that deposit-feeding gastropods, in particular *Astyris permodesta,* may temporarily enter dead zones for grazing on fresh organic detritus or sulphur bacterial filaments (Levin et al., 1991; Mosch et al., 2012). These gastropods leave small biodeformational structures on the sea bed, which are, however, usually not preserved (Schäfer, 1956). Sediments from oxygen-depleted environments are therefore characterised

by scarcity or absence of ichnofossils (Savrdaand Bottjer, 1987). Only a few ichnogenera are recognisable, in particular the mm-sized *Chondrites*. Their diameter correlates with oxygenation although food availability or substrate properties also exert an influence (Bromley and Ekdale, 1984; Fu, 1991; Kröncke, 2006). In eastern Pacific hypoxic environments, a covariance of the highest average burrow size and oxygen content of near-bottom water was recognised for an oxygen range of 5 to 45 μmol kg^{-1} in the San Pedro Basin (Savrdaet al., 1984). This relationship was based on 6 to 10 burrows identified per x-ray image. An assignment to particular ichnotaxa other than *Arenicolites* was not attempted, even though many ichnogenera have a well constrained range of dimensions (e.g. Wetzel, 2008).

The general inverse relationship of burrow diameter and oxygenation has been challenged by sea-floor observations with a photo sledge and shallow multicorer samples taken during R/V METEOR cruise M77/1 (Mosch et al., 2012). Surprisingly, it was not *Chondrites*, but centimetre-sized open crab burrows that were recognised as first biogenic structures at bottom-water oxygen concentrations approaching 10 μmol kg^{-1} close to the lower OMZ boundary where endobenthic macrofauna was able to exist. *Chondrites* burrows have not been reported to date from any of the Peruvian OMZ sediment cores even though the responsible organism, a nematod, most likely pursues chemotrophy at anaerobic conditions (Fu, 1991).

Older strata, such as Mesozoic sediments were usually subjected to a high degree of compaction altering the shape and size of burrows (e.g. Gaillard and Jautee, 2006; Gingras et al., 2010). A correct identification of ichnogenera may then not be possible any more. Burrows have been preserved at their genuine dimensions in carbonate-rich sediments (e.g. Savrda and Bottjer, 1986; Ekdale and Bromley, 1991). In particular *Chondrites*-rich layers were reported from Cenomanian/Turonian limestones and marls deposited during OAE 2 in NW Europe (Schönfeld et al., 1991; Hilbrecht and Dahmer, 1994; Rodríguez and Uchmann, 2011). As this ichnogenus is appearently missing from the Peruvian OMZ, bioturbation structures do not offer a detailed comparison between Pleistocene to recent OMZs and Cretaceous OAEs. The only feature in common is the scarcity or absence of bioturbation in both, laminated Cretaceous shales and Holocene to Pleistocene sediments deposited under dysoxic to anoxic conditions below the Peruvian upwelling.

Laminations

Laminated sediments have been studied in great detail to unravel the processes forming millimetre-scale interbedded sediments with the perspective that alternations between the varves reflect seasonal, annual or decadal environmental variability (von Stackelberg, 1972; Brodie and Kemp, 1994; Kemp, 1996). In the Arabian Sea, laminated sediments were found between 300 and 900 m water depth whereas the OMZ with oxygen concentrations of <23 µmol kg^{-1} impinges the sea floor between 200 and 1200 m depth. Minimum values of 4.5 µmol kg^{-1} were reported (Schulz et al., 1996). No benthic macroinvertebrates were observed between 300 and 800 m where these low oxygen concentrations prevailed. The laminations form couplets of dark grey organic-rich summer varves and light grey winter varves of terrigenous detritus. Holocene average sedimentation rates were in the range of 0.9 to 1.5 mm yr^{-1}. Winnowing and reworking by slope currents or turbidites was common, which prevented the establishment of continuous long records of annual resolution (Schulz et al., 1996). Instead, cyclic alternations of laminated and bioturbated core sections suggested a spatial variability of the OMZ on longer time scales (von Rad et al., 1995).

In the California borderland basins the laminae consist of dark lithogenic winter layers and light-coloured, nearly monospecific *Thalassiothrix longissima* diatom layers deposited during spring and early summer (Thunell et al., 1995). In the Soledad Basin off northern Mexico, whitish coccolith layers are intercalated as well (van Geen et al., 2003). Average sedimentation rates may exceed 1 mm yr^{-1}, and despite the pronounced seasonal or El Niño cyclicity of 3-6 years (Hagadorn, 1996), up to five biogenic sublaminae per year may be preserved (Pike and Kemp, 1997). The regional and intra-basinal distribution of laminations in latest Holocene sediments was confined to bottom-water oxygen concentrations <5 µmol kg^{-1}. In contrast, a decoupling of sediment banding and bottom-water oxygenation has been found at sites with a low primary production or where a less profound seasonality prevailed (van Geen et al., 2003). There, alterations of bioturbated glacial and stadial sediments and laminated Holocene and interstadial core sections suggested climatically driven variations in northeastern Pacific OMZ intensity (Behl and Kennett, 1996; Cannariato and Kennett, 1999; Jaccard and Galbraith, 2012).

In the Peruvian OMZ, laminated sediments from the Salaverry and Pisco Basins were described in great detail (Kemp, 1990; Wefer et al., 1990). The sediments showed 0.3 to 0.6 m thick intervals of laminated and sub-laminated sediments with intercalated homogenous

bioturbated units. They are unconformably overlain by sand-rich layers with phosphorite pebbles representing periods of erosion due to strong near-bottom currents (Reimers and Suess, 1983; Garrison and Kastner, 1990). In banded core sections, the laminae form 0.3 to 0.7 mm thick couplets of clay-rich and silt-rich layers probably reflecting depositional variability on seasonal timescales. Nearly monospecific *Skeletonema* or *Chaetoceras* diatom layers of 2 to 10 mm thickness are irregularily intercalated. These diatom ooze layers were often not preserved due to dissolution or grazing. Evidence for the latter is provided by microbioturbation within the laminated intervals and pellet-rich horizons of 5 to 30 mm thickness. These were created by epibenthic, vagile macrofauna during periods of elevated bottom-water oxygenation, which lasted for 8 to 16 years (Brodie and Kemp, 1994). A covariance of laminated core sections with certain climatic conditions was not identifiable whereas pebbly or sand-rich beds preferentially occurred during cold stages suggesting either stronger bottom currents or increased terrigenous sediment supply (Reimers and Suess, 1983; Rein et al., 2005; Mollier-Vogel et al., 2013). On decadal to subdecadal time scales, however, laminations were linked to changes in climate and ecosystem properties in the mid 19th century (Gutiérrez et al., 2006). In particular, periodical "regime shifts" in the Peruvian OMZ during the late Holocene were related to the variability of solar irradiance (Agnihotri et al., 2008).

Information on the presence of laminations is available for 74 of 136 sediment cores reported from the western South American Margin between the Equator and 18°S (Appendix Table A1). From those, 36 showed laminated intervals whereas 38 cores were homogenized by bioturbation with the exception of sediment-transport related structures, sand or gravel beds. Laminated sediment sections are confined to a distinct area between 9° and 16°S and were not retrieved from water depths below 600 m. With the exception of two cores from the continental shelf, the upper and lower distribution limits of laminated sediments match the outline of today's OMZ as depicted by the 7 μmol kg^{-1} isoline of bottom-water oxygen concentration. However, most laminated cores were retrieved from areas with bottom-water oxygen values of <5 μmol kg^{-1} (Figure 2). The distribution limits are not reliably traceable further to the North and South due to sparse data coverage and rarely observed laminated sections. Sediment records may go as far back in time as marine oxygen isotope stage 11 and contain several unconformities representing extended times of non-deposition or erosion (Rein et al., 2005).

A reliable stratigraphic record is available for 9 sediment cores with laminated intervals. Laminations occurred at any time and water depth during the past 20 kyrs with the exception of the 6 to 8 ka time interval (Figure 3). This implies that there was no period of time during the late Pleistocene and Holocene, during which the entire OMZ expanded and intensified, or contracted and weakened on a regional scale. Some of the shallowest locations showed weaker or no laminations during periods of inferred increased El Niño frequency marking seasonally decreased productivity and elevated oxygen levels in the bottom waters (Rein et al., 2005; Ehlert et al., 2013). Laminated deposits were rarely continuous and did not show a time-transgressive pattern as previously suggested (Reimers and Suess, 1983). Sections documenting periods of more than 2 kyrs duration of laminated sediment deposition were recorded only between 11 and 13°S and at water depths of 184 to 325 m, i.e. in the upper OMZ and underneath the most intense upwelling.

Organic carbon accumulation rates

Accumulation rates of sedimentary organic carbon have been widely considered as a proxy for paleoproductivity reconstructions (Stein and Stax, 1991; Sarnthein et al., 1992; McKay et al., 2004). While usually less than 1 % of organic matter exported from the photic zone is deposited on the sea floor and preserved in the fossil record under oxic conditions, the burial may increase to up to 18 % in low-oxygen environments (Müller and Suess, 1979). The preservation of organic substances in OMZ sediments from the Arabian Sea was enhanced at oxygen concentrations of <22 μmol kg^{-1} suggesting a covariance between organic carbon accumulation rates and bottom-water oxygenation (Koho et al., 2013). Recent organic carbon accumulation rates ranged from 0.01 to 0.4 g C cm^{-2} kyr^{-1} in the Arabian Sea.

In the Peruvian OMZ, mid- to late Holocene and subrecent organic carbon accumulation rates varied substantially between 0.06

and 6.8 g C cm^{-2} kyr^{-1} with most values between 1 and 3 g C cm^{-2} kyr^{-1} (Appendix Table A2), i.e. one magnitude higher than in the Arabian Sea. Dilution by seasonal terrigenous sediment input from Pakistan probably accounts for the difference (von Rad et al., 1995).

The organic carbon data from the Peruvian cores revealed distinct distribution patterns. Laminated sediments showed scattered values at bottom-water oxygen <5 μmol kg^{-1} whereas bioturbated sediments depicted a well constrained inverse relationship of organic carbon accumulation and bottom-water oxygenation (Figure 4).

~~1.2~~3.2 Organic-rich sedimentation during Cretaceous OAE-2 of the Tarfaya Basin

Laminations

The laminated intervals in sediments from the Tarfaya Basin as recovered from SN°4 well were usually 2 to 4 m thick organic-rich marlstones with intercalated bioturbated limestones of 0.5 to 2 m thickness. the laminations showed a high scatter in lightness (Figure 5), which is depicted by a lamination index based on a moving window standard deviation of high resolution lightness data (L*). Intense lamination is indicated by high standard deviations, while standard deviations in homogenous sediments are close to zero. The average thicknesses of individual laminae was extremely variable ranging from sub-millimetre (mainly light layers composed of planktonic foraminiferal tests) to several millimeters (mainly kerogen-rich dark layers). Simple estimates from average sedimentation rates of 4 to 8 cm per thousand years suggest an average time of 25 to 12.5 years to account for the deposition of a 1 mm lamina, which points to a control on lamination by depositional or winnowing processes, rather than a control by periodical climatic variations on the formation of laminae.

Wavelet spectral analyses of the 70 µm resolution linescan data of core SN°4 also do not exhibit clear periodicity patterns. The most prominent periodicities are in the range of 4, 15 and 30 mm, which would correspond to approximately 100, 400 and 800 years at a sedimentation rate of 4 cm kyr^{-1} and clearly do not reflect seasonal variability or ENSO-type sub-decadal oscillations (3-7 years) (Figure 6).

Sediment re-working and re-distribution through small scale erosion and/or winnowing by bottom currents appeared commonly in the deposition of organic-rich sediments during OAE 2. Low angle truncations, indicating small scale erosion surfaces occurred frequently in the upper part of the OAE 2 black shales in the Tarfaya Basin (i.e. in black shales at the base of the Turonian within the Amma Fatma outcrop section, Figure 7).

Recent depositional environments off NW Africa were distinctly different from those during OAE 2. In the modern upwelling zone off NW Africa, textural upwelling indicators, such as organic-rich, laminated sediments, were virtually absent in shallow shelf sediments directly underlying upwelling cells (Fütterer, 1983). They were winnowed out by strong bottom currents, sediment particles were transported across the shelf and finally redeposited in deeper parts of the shelf or on the continental slope. The main depositional center of organic-rich

material is located today at water depths between 1000 and 2000 m, where fine-grained material is accumulating as mid-slope mud lenses (Sarnthein et al., 1982).

The organic-rich sediments in the Cretaceous Tarfaya Basin also exhibited a range of sedimentary features pointing to an important role of re-suspension and lateral advection in the depositional processes. However, sedimentological (El Albani et al., 1999) and micropaleontological evidences (Wiedmann et al., 1978; Gebhardt et al., 2004, Kuhnt et al., 2009) indicated that the main depositional center of organic-rich sediments during OAE 2 were in the middle to outer shelf part of the Tarfaya Basin in relatively shallow water depths between approx. 100 and 300 m. Such a setting would be in general agreement with the situation on the Peruvian shelf and upper slope today, where similar high-accumulation areas were recognised at depths of less than 300m (Wefer et al., 1990).

Organic carbon accumulation rates during OAE 2 in the Tarfaya Basin

Organic matter accumulation rates were calculated in three cores (S13, S75, SN°4) for individual cycles based on an orbitally tuned age model (Meyers et al., 2012) for the time interval from the onset of OAE 2 (late Cenomanian, upper part of the *R. cushmani* Zone) to the lower Turonian (end of the OAE 2 carbon isotope excursion in the *H. helvetica* Zone). This period represents a time span of ~ 800 kyr (Sagemann et al., 2006; Meyers et al., 2012).

Cores were correlated using density and natural gamma ray logs. We used density/NGR minima/maxima for each individual cycle as tie points, and, whenever possible, correlatable features within individual cycles. The overall pattern and number of cycles in the studied interval revealed that most of the regular density variations mirrored obliquity cycles, i.e. a periodicity of 41 kyrs. The local cyclostratigraphic age model is then tied to the GTS2012 timescale chronology using the new radiometric age of 93.9 Ma for the C/T boundary (top cycle 3, FO *Quadrum gartneri*). Based on this age model, we calculated sedimentation rates for each individual cycle, dry bulk density from density logging and total organic carbon values from individual measurements as well as continuous organic carbon estimates from NGR logging and lightness (L*) measurements (Figure 8).

4 Discussion

4.1 Origin and composition of laminae

Light laminae in Peruvian upwelling sediments represent diatom blooms, either resulting from seasonal variations or deposition during strong La Niña events (Kemp, 1990), whereas in the Tarfaya Basin light layers are mainly composed of planktonic foraminiferal tests, phosphate or fecal pellets, indicating periods of higher oxygenation of the water column with enhanced grazing activity of vagile benthic organisms. These events occurred on decadal-centennial timescales as brief interruptions of otherwise continuously dysoxic to anoxic conditions.

The different marine primary producers in the Cenomanian-Turonian may have influenced the stoichiometry and isotope composition of marine organic matter. Whereas Holocene to Recent organic-rich sediments in the Peruvian upwelling contain high proportions of diatoms, Cretaceous organic-rich sediments are dominated by haptophyte algae preserved as shields of coccolithophorids and nannoconids, archaeans, and cyanobacteria as revealed by biomarkers (Kuypers et al. 1999; Dumitrescu and Brassell, 2005). It is conceivable that such organisms may have induced higher C/P and C/N ratios under high pCO_2 conditions, exceeding the Redfield ratio (Sterner and Elser, 2002; Riebesell, 2004; Sterner et al., 2008; Flögel et al., 2011; Hessen et al., 2013). As a result, nutrient limitation for marine productivity may have been less severe during Cretaceous OAEs, than it was reached under low pCO_2 conditions during the last deglaciation and the Holocene.

~~1.2~~4.2 Persistence of laminated sediments – dynamics of the OMZ

The geological record of OAE 2 in the Tarfaya Basin showed a cyclic sedimentation of variegated, laminated marlstone beds with low gamma-ray density and high organic carbon accumulation rates, which were intercalated with uniformly pale, bioturbated limestones showing low organic carbon values. A regular periodicity of cyclic sedimentation in the obliquity domain indicated climatic forcing that was different from Late Cretaceous times with well-ventilated oceans, when short and long precession, and eccentricity had a stronger influence (Gale et al., 1999; Voigt and Schönfeld, 2010). It has been suggested that changes in mid-depth ocean circulation during OAE 2 promoted the influence of a high-southern latitude climatic signal in the Cretaceous North Atlantic (Meyers et al., 2012).

In the north-eastern Pacific, we also see alterations of bioturbated sediments deposited during the last glacial and stadial climatic intervals with laminated intervals deposited during the Holocene and late Pleistocene interstadials (Behl and Kennett, 1996; Cannariato and Kennett, 1999). Even though these alterations reflect much shorter periodicities than during the mid Cretaceous, they were climatically driven by intensified upwelling due to stronger trade winds and enhanced nutrient supply through Subantarctic Mode Water, thus again linked to processes in the Southern Ocean (Jaccard and Galbraith, 2012, and references therein).

Off Peru, laminations have neither been strictly linked to climatic periodicities nor were they continuously preserved in the fossil record. Numerous discontinuities, their time-transgressive nature, and phosphoritic sand layers are evidences for the impact of strong bottom-near currents and breaking internal waves (Reimers and Suess, 1983). On the other hand, eddies and warm, oblique filaments can facilitate a short-term supply of oxygen to the Peruvian OMZ (e.g. Stramma et al., 2013), and large burrowing or grazing organisms may invade the dead zone from below (Mosch et al., 2012), thus destroying recently deposited laminae. Therefore it is conceivable that a preservation of continuous laminated sediments has rather been an exception than the rule in the Peruvian OMZ. This exception was more likely to occur in the permanently anoxic centre of the OMZ underneath the most intense upwelling cell.

None-the-less, it has to be emphasized that many of the north-eastern Pacific cores were retrieved from marginal basins where a quiet depositional regime prevailed. Furthermore, the impact of bottom-near currents and redeposition is also documented in OAE 2 deposits from Tarfaya outcrop sections. We speculate that if there were a possibility to examine older Peruvian OMZ sediments in an outcrop section, many similar features will emerge helping to better understand the fragmentations of the stratigraphic record described above.

~~1.3~~4.3 Organic carbon accumulation and bottom-water oxygenation

A large range of chemical, biological and oceanographic factors controlling organic detritus flux to the sea bed, decomposition and remineralisation, preservation and finally accumulation as refractory substances constitute the complex nature of organic matter turnover. Furthermore, organic carbon preservation strongly depends on the local circumstances of deposition (Hedges and Keil, 1995; Arndt et al., 2013), thus limiting the comparability of settings between regions and oceanic basins. There is an ongoing debate

whether the proportion of organic matter, which is buried and preserved in marine sediments, is dependant on the ambient bottom water oxygenation or not (Dale et al., 2014). The only assured perception is that carbon burial does not co-vary with bottom-water oxygenation at high sedimentation rates near continental margins (Betts and Holland, 1991; Canfield, 1994). At low sedimentation rates, the oxygenated near-surface layer of sediments deposited under oxygenated bottom water increases in thickness and faciltates enhanced aerobic decomposition, while sediments deposited under low-oxic conditions remain anaerobic and decomposition is effected by nitrate and sulphate reduction (Hartnett and Devol, 2003). As a consequence, organic carbon burial correlates with oxygen exposure time of particulate organic carbon at the sea floor in oxic to suboxic environments, and shows no covaraince in dysoxic zones (Hartnett et al. 1998).

~~1.~~4.4 Comparison of organic carbon accumulation rates: Glacial-Holocene Peruvian upwelling vs. Cretaceous upwelling along the East Atlantic Margin

For a comparison of Cretaceous organic carbon accumulation rates with those of Recent OMZs, we considered Cretaceous sections with more than 90% organic rich shales (Kuhnt et al., 1990). With reference to Recent OMZ sediments, we assumed a bottom water oxygenation <5 µmol kg^{-1} at sites where fine laminations were preserved. The first estimates of TOC accumulation rates of Kuhnt et al. (1990) were based on a duration of 500 kyr for OAE 2 and on averaging of a relatively small number of discrete organic carbon measurements over the entire interval. These rough estimates resulted in accumulation rates between 0.01 g C cm^{-2} kyr^{-1} for deep sea sites and 1.1 g C cm^{-2} kyr^{-1} for NW African shelf basins with upwelling conditions, which showed the highest accumulation rates (Kuhnt et al., 1990). A re-evaluation of organic carbon accumulation rates in the Tarfaya Basin using an orbitally tuned age model and high resolution measurements or continuous organic carbon estimates indicated variable carbon accumulation rates, which varied between 0.7 and 2.8 g C cm^{-2} kyr^{-1} and thus match the data range of the majority of laminated late Holocene sediments from the Peruvian margin presently under bottom-water oxygen levels of <5 µmol kg^{-1} (Figure 4).

The palaeo water depths of the Tarfaya Basin during OAE 2 were slightly shallower than the centre of the Peruvian OMZ today. Based on molecular evidences, it was even suggested that the Cretaceous OMZ extended into the photic zone (Sinninghe Damsté and Köster, 1998). As

such, decomposition and remineralisation of organic detritus while sinking to the sea floor was less likely (Martin et al., 1987). We therefore have to assume that the deposition rate of particulate organic matter was very close to the export flux at 150 m water depth (Buesseler et al., 2007). An empirical relationship between the rain rate and Holocene burial rate of particulate organic carbon has been established by Flögel et al. (2011) for continental margin settings:

$$\textit{Eq. 1: } BUR_{POC} = 0.14 * RR_{POC}^{1.1}$$

(BUR_{POC} = burial rate of particulate organic carbon; RR_{POC} = rain rate of particulate organic carbon)

No significant difference between data from oxygen minimum zones and well-ventilated bottom waters is recognised (Flögel et al., 2011, their Figure 2). Applying Equation 1 and considering a maximum organic carbon accumulation rate of 2.8 g C cm^{-2} kyr^{-1}, i.e. approximately 30 g C m^{-2} yr^{-1} to bring up to a round figure, the maximum paleo rain rate would be on the order of 126 g C m^{-2} yr^{-1}, i.e. about half the productivity of the present day Peruvian upwelling provides ranging from 200 to >400 g C m^{-2} yr^{-1} (Wefer et al., 1983). Even though this approximation includes many uncertainties, e.g. reliability of early sediment traps, variable burial efficiency (Dale et al., 2014), poorly constrained rates of Cretaceous primary production, it is reasonable to assume that part of the OAE 2 organic matter was lost during early diagenesis.

It has to be emphasized that Holocene organic carbon accumulation rates in the centre of the Peruvian OMZ show a large scatter too, with maximum values of 6.8 g C cm^{-2} kyr^{-1} in core SO147-106KL, i.e. rounded up 70 g C m^{-2} yr^{-1}. If we likewise apply Equation 1, we obtain a rain rate of 270 g C m^{-2} yr^{-1}. This value is in good agreement with today's productivity of the Peruvian upwelling, and it is derived from a core interval, where an unusually thick section of laminations was preserved. None-the-less, the Recent carbon burial efficiency at 10 cm sediment depth close to the SO147-106KL coring site amounts to 62 % of the organic matter arriving at the sea floor (Dale et al., 2014). It is thus much higher than burial rate estimates for the late Holocene (Müller and Suess, 1979). The difference may either originate from a strong inter-annual variability, a subrecent rise in carbon accumulation since 1800 AD (Gutierrez et al., 2009), or for a further remineralisation of organic matter with time in the historical layer below 10 cm sediment depth and beyond.

For the laminated beds of OAE 2 in the Tarfaya Basin, a bottom water oxygenation of less than 5 µmol kg^{-1} is suggested with reference to the distribution of laminated sediments in Recent oxygen minimum zones worldwide. The question arises whether it is possible to assign a bottom-water oxygen estimate to the intercalated, pale bioturbated limestones from the Tarfaya sections. Indeed, benthic foraminifera from the non-laminated light coloured interval at the base of cycle 0 in core S75 revealed a diverse benthic foraminiferal assemblage dominated by *Bolivina* species in high abundances. They indicate less dysoxic bottom waters (Kuhnt et al., 2005). The organic carbon accumulation rate was estimated at 1.1 g C cm^{-2} kyr^{-1} over this interval. If we apply the late Holocene relationship of organic carbon accumulation rates and bottom water oxygen for bioturbated sediments, an oxygenation of ca. 38 µmol kg^{-1} is obtained. Such levels prevail at the Peruvian Margin today either below 800 m water depth, i.e. well below the OMZ, or above 90 m depth in the surface ocean mixed layer. *Bolivina* dominated faunas live in the centre of the Peruvian OMZ today, with high abundances between 150 and 520 m, and at oxygen concentrations of <2 µmol kg^{-1} (Mallon, 2012). Between 800 and 900 m depth, the range to which the Cretaceous oxygen approximation points, *Bolivina* species were rare, accounting for less than 5 % of the living fauna.

5 Conclusions

Pleistocene to Holocene and late Cenomanian to early Turonian stages are more than 94 million years apart in Earth's history. A direct comparison of their sedimentary record and environmental processes is hampered by burial diagenesis, evolution of marine biota, different continental and ocean configuration, different climate, ocean circulation, and biogeochemical cycles. The late Cenomanian was marked by the onset of OAE 2. Sedimentological, faunistic, and biogeochemical parameters suggested that large parts of the water column were devoid of dissolved oxygen, but the absolute levels are less well constrained. In an actualistic approach, we compared deposits of OAE 2 from the Moroccan shelf close to Tarfaya with deglacial and Holocene OMZ sediments from the upwelling area off Peru and found only a few parameters for a reliable investigation of paleo low-oxygen conditions in both records, i.e. trace fossils, laminations, and organic carbon accumulation rates.

The millimetre-sized trace fossil *Chondrites* was common in Cretaceous strata, in particular in the beds directly underlying OAE 2 black shales. It was also found in modern oxygen-

depleted environments, where it is created by a nematod pursuing chemotrophy at anaerobic conditions. The burrow diameter increased with oxygen level from 5 to 45 µmol kg^{-1} in the San Pedro Basin, California. However, *Chondrites* has never been reported from Peruvian OMZ sediments. The oxygen - burrow size relationship is challenged by cm-sized crab burrows appearing at oxygen levels around 10 µmol kg^{-1} below the OMZ already. Crab burrows are also common in Cretaceous sediments. Their appearence in OAE 2 sediments may therefore indicate that a threshold of approximately 10 µmol kg^{-1} bottom-water oxygen has been exceeded.

Laminations are a more reliable indicator, but they display only one, very low oxygen level. In the Peruvian, northeastern Pacific, and Pakistan OMZs, depositional laminae created by seasonal or multi-annual variations in sediment supply or composition were preserved at bottom-water oxygen concentrations of less than 5 µmol kg^{-1}. Coherent occurrences of laminated beds and biogeochemical indicators for oxygen drawdown in Tarfaya OAE 2 sediments supported the applicability of this feature for bottom-water oxygen estimates. The cyclic pattern of laminated and non-laminated intervals in Tarfaya sections and in sediment cores from the eastern Pacific suggested the impact of climatic variations with direct linkages to the high-latitude Southern Ocean as source of nutrients and better ventilated intermediate waters. This regular cyclic pattern is blurred in Peruvian OMZ sediments by erosion, omission and redeposition due to bottom-near currents and breaking internal waves, making the preservation of laminated sediments an exception rather than the rule. Redeposition features were also observed in Tarfaya outcrop sections and reveal episodic, strong currents on the Cretaceous shelf and upper slope as an important process that was likely responsible for many observed unconformities in upper Cenomanian and lower Turonian formations.

Organic carbon accumulation rates of late Holocene sediments off Peru displayed a disjunct pattern. They showed a high scatter and a broad abundance maximum between 0.8 und 2.8, mode value at 1.3 µmol kg^{-1}, in laminated sediments under a Recent bottom-water oxygenation of <5 µmol kg^{-1}. If we compare the carbon accumulation rates of the Tarfaya OAE 2 laminated sediments with late Holocene to Recent ones from the Peruvian OMZ, the Cretaceous rates between 0.7 and 2.8 g C cm^{-2} kyr^{-1} match the data range of the majority of late Holocene sediments very well. Taking into account the high burial efficiency of organic carbon deposited in OMZs, and calculating deposition fluxes from the photic zone, the maximum Cretaceous values would account for only half of the present-day export production

under the Peruvian upwelling. Thermal maturation or the loss of volatile hydrocarbons from Tarfaya black shales may well account for this difference. Maximum Holocene carbon accumulation rates off Peru compare well to the present-day export production. This agreement is, however, valid only for sediments with a continuous, laminated record. All other cores exhibiting average carbon accumulation rates have most likely been subjected to instant winnowing and redeposition of organic detritus.

At higher oxygen levels, organic carbon accumulation rates showed an inverse exponential relationship with oxygen concentrations. This mirrors the successive bioirrigation and concomittant decomposition of organic matter through increasingly better ventilation below the Peruvian OMZ. Such a relationship has not been described before. Few available data from the Arabian Sea suggested a similar covariance conferring credibility to the pattern observed at the Peruvian margin (Koho et al., 2013). The relationship has been used to assign a paleo oxygen level to a well constrained, intermittently oxygenated interval at the base of cycle 0 (named Plenus Cold Event) in the Tarfaya sections. The estimate of 38 μmol kg^{-1} overall disagrees with the composition of the Cretaceous and Recent benthic foraminiferal assemblages prevailing at this oxygen level.

In summary, close similarities and distinct differences between the two periods of low oxygenation in the sedimentary record of the Cretaceous OAE2 and the Late Quaternary OMZs were recognised. More data are needed to further constrain the organic carbon accumulation – oxygen relationship. This emerging paleoproxy has to becomplemented and corroborated by other, advanced bottom-water ventilation proxies, e.g. molybdenum isotopes or I/Ca ratios in foraminiferal shells in order to achieve more quantitative reconstructions of past oxygen levels and their controlling factors.

Acknowledgements

Stefan Sommer, Thomas Mosch, and Richard Camilli, Kiel, operated the CTD during R/V METEOR cruise M77-1 and provided the water column oxygen profiles. Samuel Jaccard, Bern, provided previously unpublished data on Pacific sediment cores, and Ralph Schneider, Kiel, provided core photographs obtained during R/V METEOR M77/2 cruise. Marcus Dengler and Kristin Döring, Kiel, gave advise about primary production and mid-depth hydrodynamics at the Peruvian Margin. Volker Liebetrau, Kiel, scrutinised an earlier draft of this paper. Their support, encouragements, and suggestions are greatfully acknowledged. We thank the Associate Editor Christophe Rabouille, Holger Gebhardt, and an anonymous

reviewer for their useful and constructive comments. The corresponding author thanks the Subcommission on Cretaceous Stratigraphy, Germany, for intense discussions on OAE 2 features and dynamics during their excursions to unnumbered outcrop sections. This work was funded by Deutsche Forschungsgemeinschaft (DFG) through SFB 754 “Climate–Biogeochemistry Interactions in the Tropical Ocean”.

References

Agnihotri, R., Altabet, M.A., Herbert, T.D., Tierney, J.E.: Subdecadally resolved paleoceanography of the Peru margin during the last two millennia, Geochem., Geophy., Geosy. 9, 1525-2027, doi: 10.1029/2007GC001744, 2008.

Anbar, A.D., Rouxel, O.: Metal Stable Isotopes in Paleoceanography, Annual Review of Earth Planet. Sci., 35, 717-746, doi: 10.1146/annurev.earth.34.031405.125029, 2007.

Aquit, M., Kuhnt, W., Holbourn, A., Chellai, E.H., Stattegger, K., Kluth, O., Jabour, H.: Late Cretaceous paleoenvironmental evolution of the Tarfaya Atlantic coastal basin, SW Morocco, Cretaceous Res. 45, 288–305, doi: 10.1016/j.cretres.2013.05.004, 2013.

Arndt, S., Jørgensen, B.B., LaRowe, D.E., Middelburg,J.J., Pancoste,R.D., Regnier, P.: Quantifying the degradation of organic matter in marine sediments: A review and synthesis. Earth-Science Rev., 123, 53–86, doi:10.1016/j.erscirev.2013.02.008, 2013.

Behl, R.J., Kennett, J.P.: Brief interstadial events in the Santa Barbara Basin, NE Pacific, during the past 60 kyr, Nature, 379, 243-246, doi: 10.1038/379243a0, 1996.

Betts, J.N., Holland, H.D.: The oxygen content of ocean bottom waters, the burial effciency of organic carbon, and the regulation of atmospheric oxygen. Palaeogeogr,, Palaeoclimatol,, Palaeoecol., 97, 5–18, doi:10.1016/0921-8181(91)90123-E, 1991

Böning, P., Brumsack, H.J., Böttcher, M.E., Schnetger, B., Kriete, C., Kallmeyer, J., Borchers, S.L.: Geochemistry of Peruvian near-surface sediments, Geochim. Cosmochim. Acta, 68, 4429-4451, doi:/10.1016/j.gca.2004.04.027, 2004.

Boyce, R.E.: Definitions and laboratory techniques of the compressional sound velocity parameters and wet-water content, wet-bulk density and porosity parameters by gravimetric and gamma-ray attenuation techniques, Initial Rep. Deep Sea Drilling Project, 33, 931-958, 1976.

Brodie, I., Kemp, A.E.S.: Variation in biogenic and detrital fluxes and formation of laminae in late Quaternary sediments from the Peruvian coastal upwelling zone, Mar. Geol. 116, 385-398, doi: 10.1016/0025-3227(94)90053-1, 1994.

Bromley, R.G., Ekdale, A.A.: Chondrites: a trace fossil indicator of anoxia in sediments, Science, 224, 872-874, doi: 10.1126/science.224.4651.872, 1984.

Brumsack, H.J.: The trace metal content of recent organic carbon-rich sediments: Implications for Cretaceous black shale formation, Palaeogeogr., Palaeoclimatol., Palaeoecol., 232, 344-361, doi:10.1016/j.palaeo.2005.05.011, 2006.

Buesseler, K.O., Lamborg, C.H., Boyd, P.W., Lam, P.J., Trull, T.W. Bidigare, R.R., Bishop, J.K.B. Casciotti, K.L., Dehairs, F., Elskens, M., Honda, M., Karl, D.M., Siegel, D.A., Silver, M.W., Steinberg, D.K., Valdes, J., Van Mooy, B., Wilson, S.: Revisiting Carbon Flux Through the Ocean's Twilight Zone, Science, 316, 567, doi: 10.1126/science.1137959, 2007.

Buggisch, W.: The global Frasnian-Famennian »Kellwasser Event«, Geol. Rundsch. 80, 49-72, doi: 10.1007/BF01828767, 1991.

Calvert, S.E.: Oceanographic controls on the accumulation of organic matter in marine sediments, Geol. Soc. S.P. 26, 137-151, doi: 10.1144/GSL.SP.1987.026.01.08, 1987.

Canfield, D.E.: Factors influencing organic carbon preservation in marine sediments. Chemical Geology, 114, 315-329, doi:10.1016/0009-2541(94)90061-2, 1994.

Cannariato, K.G., Kennett, J.P.: Climatically related millennial-scale fluctuations in strength of California margin oxygen-minimum zone during the past 60 k.y., Geology, 27, 975-978, doi: 10.1130/0091-7613, 1999.

Dale, A.W., Meyers, S.R., Aguilera, D.R., Arndt, S., Wallmann, K.: Controls on organic carbon and molybdenum accumulation in Cretaceous marine sediments from the Cenomanian–Turonian interval including Oceanic Anoxic Event 2. Chem. Geol., 324-325, 28-45, doi: 10.1016/j.chemgeo.2011.04.014, 2012.

Dale, A.W., Sommer, S., Lomnitz, U., Montes, I., Treude, T., Gier, J., Hensen, C., Dengler, M., Stolpovsky, K., Bryant, L.D., Wallmann, K.: Organic carbon production, mineralization and preservation on the Peruvian margin. Biogeosciences Discuss., 11, 13067-13126, doi:10.5194/bgd-11-13067-2014, 2014.

Dumitrescu, M., Brassell, S.C.: Biogeochemical assessment of sources of organic matter and paleoproductivity during the early Aptian Oceanic Anoxic Event at Shatsky Rise, ODP Leg 198, Org. Geochem., 36, 1002-1022, doi:10.1016/j.orggeochem.2005.03.001, 2005.

Ehlert, C., Grasse, P., Frank, M.: Changes in silicate utilisation and upwelling intensity off Peru since the Last Glacial Maximum – insights from silicon and neodymium isotopes, Quaternary Sci. Rev., 72, 18-35, doi: 10.1016/j.quascirev.2013.04.013, 2013.

Einsele, G., Wiedmann, J.: Faunal and sedimentological evidence for upwelling in the Upper Cretaceous coastal basin of Tarfaya, Morocco, Ninth Internat. Congress of Sedimentology, Nice, theme vol. 1, 67-72, 1975.

Ekdale, A.A., Bromley, R.G.: Analysis of composite ichnofabrics: an example in uppermost Cretaceous chalk of Denmark, Palaios, 6, 232-249, 1991.

El Albani, A., Kuhnt, W., Luderer, F., Caron, M.: Palaeoenvironmental evolution of the Late Cretaceous sequence in the Tarfaya Basin (southwest of Morocco), Geol. Soc. S.P., 153, 1, 223–240, 10.1144/GSL.SP.1999.153.01.14, 1999.

EPICA Community Members: One-to-one coupling of glacial climate variability in Greenland and Antarctica, Nature, 444, 195-198, doi: 10.1038/nature05301, 2006.

Erbacher, J., Huber, B.T., Norris, R.D., Markay, M.: Increased thermohaline stratification as a possible cause for an ocean anoxic event in the Cretaceous period, Nature 409, 325-327, doi: 10.1038/35053041, 2001.

Flögel, S., Wallmann, K., Poulsen, C. J., Zhou, J., Oschlies, A., Voigt, S., Kuhnt, W.: Simulating the biogeochemical effects of volcanic CO2 degassing on the oxygen-state of the deep ocean during the Cenomanian/Turonian Anoxic Event (OAE2), Earth Planet. Sci. Lett., 305, 371-384, doi:10.1016/j.epsl.2011.03.018, 2011.

Flower, B.P., Kennett, J.P.: Relations between Monterey Formation deposition and middle Miocene global cooling: Naples Beach section, California, Geology, 21, 877-880, doi: 10.1130/0091-7613, 1993.

Fu, S.: Funktion, Verhalten und Einteilung fucoider und lophocteniider Lebensspuren. Courier Forsch. Senck., 125, 1-79, 1991.

Fütterer, D.K.: The modern upwelling record off northwest Africa, in: Coastal Upwelling – its sedimentary record Part B: Sedimentary Records of Ancient Coastal Upwelling, edited by: Thiede, J., Suess, E., NATO Conference Series IV: Mar. Sci., Vol. 10b, 105-122, 1983.

Gaillard, C., Jautee, E.: The use of burrows to detect compaction and sliding in fine-grained sediments: an example from the Cretaceous of S.E. France, Sedimentology, 34, 585-593, doi: 10.1111/j.1365-3091.1987.tb00788.x, 2006.

Gale, A.S., Hancock, J.M., Kennedy, W.J.: Biostratigraphical and sequence correlation of the Cenomanian successions in Mangyshlak (W. Kazakhstan) and Crimea (Ukraine) with those in southern England, Bull. Inst. R. Sc. N. B.-S., 69, Supp. A, 67–86, 1999.

Garrison, R.E., Kastner, M.: Phosphatic sediments and rocks recovered from the Peru margin during ODP Leg 112, in: Proceedings Ocean Drilling Program, Scientific Results, edited by: Suess, E., Huene, R., et al., Vol. 112, 111-134, 1990.

Gebhardt, H., Kuhnt, W., Holbourn, A.: Foraminiferal response to sealevel change, organic flux and oxygen deficiency in the Cenomanian of the Tarfaya Basin, southern Morocco, Mar. Micropaleontol. 53, 133-158, doi: 10.1016/j.marmicro.2004.05.007, 2004.

Gingras, M.K., MacEachern, J.A., Dashtgard, S.E.: Using process ichnology to refine interpretations of sedimentary rocks, GeoCanada 2010, Abstract 680, 2010.

Gutiérrez, D., Sifeddine, A., Reyss, J.L., Vargas, G., Velazco, F., Salvatteci, R., Ferreira, V., Ortlieb, L., Field, D., Baumgartner T., Boussafir M., Boucher H., Valdés, J., Marinovic, L., Soler, P., Tapia, P.: Anoxic sediments off Central Peru record interannual to multidecadal changes of climate and upwelling ecosystem during the last two centuries, Advances Geosci., 6, 119-125, doi:10.5194/adgeo-6-119-2006, 2006.

Gutiérrez, D., Sifeddine, A., Field, D. B., Ortlieb, L., Vargas, G., Chávez, F. P., Velazco, F., Ferreira, V., Tapia, P., Salvatteci, R., Boucher, H., Morales, M. C., Valdés, J., Reyss, J.-L., Campusano, A., Boussafir, M., Mandeng-Yogo, M., García, M., and Baumgartner, T.: Rapid reorganization in ocean biogeochemistry off Peru towards the end of the Little Ice Age, Biogeosciences, 6, 835–848, doi:10.5194/bg-6-835-2009, 2009.

Hagadorn, J.W.: Laminated sediments of Santa Monica Basin, California Continental Borderland, Geol. Soc. S.P. 116, 111-120 doi: 10.1144/GSL.SP.1996.116.01.11, 1996.

Hartnett, H.E., Devol, A.H. Role of a strong oxygen-deficient zone in the preservation and degradation of organic matter: a carbon budget for the continental margin of northwest Mexico and Washington State. Geochim. Cosmochim. Acta, 67 , 2., 247–264, doi:10.1016/S0016-7037(02)01076-1, 2003.

Hartnett, H.E., Keil, R.G., Hedges, J.I., Devol, A.H.: Influence of oxygen exposure time on organic carbon preservation in continental margin sediments. Nature, 391, 572–574, doi:10.1038/35351, 1998.

Hedges, J.I., Keil, R.G.: Sedimentary organic matter preservation: an assessment and speculative synthesis, Mar. Chem, 49, 81-115, doi:10.1016/0304-42303(95)00008-f, 1995.

Helly, J.J., Levin, L.A.: Global distribution of naturally occurring marine hypoxia on continental margins, Deep-Sea Res. PTI 51, 1159-1168, doi: 10.1016/j.dsr.2004.03.009, 2004.

Herrle, J.O., Kößler, P., Friedrich, O., Erlenkeuser, H., Hemleben, C.: High-resolution carbon isotope records of the Aptian to Lower Albian from SE France and the Mazagan Plateau (DSDP Site 545): a stratigraphic tool for paleoceanographic and paleobiologic reconstruction, Earth Planet. Sci. Lett. 218, 149–161, doi: 10.1016/S0012-821X(03)00646-0, 2004.

Hesselbo, S.P., Grocke, D.R., Jenkyns, H.C., Bjerrum, C.J., Farrimond, P., Morgans Bell, H.S., Green, O.R.: Massive dissociation of gas hydrate during a Jurassic oceanic anoxic event, Nature, 406, 392-395, doi:10.1038/35019044, 2000.

Hessen, D.O., Elser, J.J., Sterner, R.W., Urabe, J.: Ecological stoichiometry: An elementary approach using basic principles, Limnol. Oceanogr., 58, 2219–2236, doi: 10.4319/lo.2013.58.6.2219, 2013.

Hetzel, A., Böttcher, M.E., Wortmann, U.G., Brumsack, H.J.: Paleo-redox conditions during OAE 2 reflected in Demerara Rise sediment geochemistry (ODP Leg 207), Palaeogeogr., Palaeoclimatol., Palaeoecol., 273, 302-328, doi:10.1016/j.palaeo.2008.11.005, 2009.

Hilbrecht, H., Dahmer, D.D.: Sediment dynamics during the Cenomanian-Turonian (Cretaceous) oceanic anoxic event in Northwestern Germany, Facies, 30, 63-83, doi: 10.1007/BF02536890, 1994.

Imbrie, J., Hays, J., Martinson, D., Mclntyre, A., Mix, A., Morley, J., Pisias, N., Prell, W., and Shackleton, N.: The orbital theory of Pleistocene climate: support from a revised chronology of the marine 5180 record. In Berger, A., Imbrie, J., Hays, J., Kukla, G., and Saltzman, B. (Eds.), Milankovitch and Climate. Part 1: Dordrecht (Riedel), doi:269-305. 10.1007/978-94-017-4841-4, 1984.

Jaccard, S.L., Galbraith, E.D.: Large climate-driven changes of oceanic oxygen concentrations during the last deglaciation, Nat. Geosci. 5, 151-156, doi:10.1038/ngeo1352, 2012.

Jenkyns, H.C., Gale, A.S., Corfield, R.M.: Carbon- and oxygen-isotope stratigraphy of the English Chalk and Italian Scaglia and its palaeoclimatic significance, Geol. Mag. 131, 1–34, doi: 10.1017/S0016756800010451, 1994.

Joachimski, M.M., Pancost, R.D., Freeman, K.H., Ostertag-Henning, C., Buggisch, W.: Carbon isotope geochemistry of the Frasnian–Famennian transition, Palaeogeogr. Palaeoclimatol. Palaeocl., 181, 91-109, doi: 10.1016/S0031-0182(01)00474-6, 2002.

Kalvelage, T., Lavik, G., Lam, P., Contreras, S., Arteaga, L., Löscher, C. R., Oschlies, A., Paulmier, A., Stramma, L., Kuypers, M. M. M.: Nitrogen cycling driven by organic matter export in the South Pacific oxygen minimum zone, Nat. Geosci., 6, 228-234, doi: 10.1038/ngeo1739, 2013.

Kemp, A.E.S.: Sedimentary fabrics and variation in lamination style in Peru continental margin upwelling sediments, in: Proceedings Ocean Drilling Program, Scientific Results, edited by: Suess, E., Huene, R., et al., Vol. 112, 43-58, 1990.

Kemp, A.E.S. (ed.): Palaeoclimatology and Palaeoceanography from laminated sediments, Geol. Soc. S.P. 116, 252 p., 1996.

Koho, K.A., Nierop, K.G.J., Moodley, L., Middelburg, J.J., Pozzato, L., Soetaert, K., van der Plicht, J., Reichart, G-J.: Microbial bioavailability regulates organic matter preservation in marine sediments, Biogeosciences, 10, 1131-1141, doi: 10.5194/bg-10-1131-2013, 2013.

Kolonic, S., Wagner, T., Forster, A., Sinninghe Damsté, J.S., Walsworth-Bell, B., Erba, E., Turgeon, S., Brumsack, H.J., Chellai, E.H., Tsikos, H., Kuhnt, W., Kuypers, M.M.M.: Black shale deposition on the northwest African Shelf during the Cenomanian/Turonian oceanic anoxic event: Climate coupling and organic carbon burial, Paleoceanography, 20, doi: 10.1029/2003PA000950, 2005.

Krahmann, G.: Physical oceanography during METEOR cruise M77/2, IFM-GEOMAR Leibniz-Institute of Marine Sciences, Kiel University, doi:10.1594/PANGAEA.778021, 2012.

Kröncke, I.: Structure and function of macrofaunal communities influenced by hydrodynamically controlled food availability in the Wadden Sea, the open North Sea, and the deep-sea: a synopsis, Senck. Marit., 36, 123-164, doi: 10.1007/BF03043725, 2006.

Kuhlbrodt, T., Griesel, A., Montoya, M., Levermann, A., Hofmann, M., Rahmstorf, S.: On the driving processes of the Atlantic meridional overturning circulation, Rev. Geophys., 45, doi: 10.1029/2004RG000166, 2007.

Kuhnt, W., Chellai, H., Holbourn, A., Luderer, F., Thurow, J., Wagner, T., El Albani, A., Beckmann, B., Herbin, J.P., Kawamura, H., Kolonic, S., Nederbragt, S., Street, C., Ravilious, K.: Morocco Basin's sedimentary record may provide correlations for Cretaceous paleoceanographic events worldwide, Eos, 82, 33, 361-368, doi: 10.1029/01EO00223, 2001.

Kuhnt, W., Herbin, J.P., Thurow, J., Wiedmann, J.: Distribution of Cenomanian-Turonian Organic Facies in the Western Mediterranean and along the Adjacent Atlantic Margin, in: Deposition of Organic Facies, edited by: Huc, A.Y., AAPG Stud. Geol., 30, 133-160, 1990.

Kuhnt, W., Holbourn, A., Gale, A., Chellai, E.H., Kennedy, W.J.: Cenomanian sequence stratigraphy and sea-level fluctuations in the Tarfaya Basin (SW Morocco), Bull. Geol. Soc. Am., 121, 11–12, doi: 10.1130/B26418.1, 2009.

Kuhnt, W., Luderer, F., Nederbragt, S., Thurow, J., Wagner, T.: Orbital-scale record of the Late Cenomanian-Turonian oceanic anoxic event (OAE-2) in the Tarfaya Basin (Morocco), Int. J. Earth Sci., 94, 147–159, doi: 10.1007/s00531-004-0440-5, 2005.

Kuhnt, W., Nederbragt, A., Leine, L.: Cyclicity of Cenomanian-Turonian organic-carbon-rich sediments in the Tarfaya Atlantic Coastal Basin (Morocco), Cretaceous Res., 18, 587–601, doi: 10.1006/cres.1997.0076, 1997.

Kuypers, M.M.M., Pancost, R.D., Sinninghe Damsté, J.S.: A large and abrupt fall in atmospheric CO_2 concentration during Cretaceous times, Nature, 399, 342-345, doi:10.1038/20659, 1999.

Leine, L.: Geology of the Tarfaya oil shale deposit, Morocco, Geol. Mijnbouw, 65, 57–74, 1986.

Levin, L.A., Huggett, C.L., Wishner, K.F.: Control of deep-sea benthic community structure by oxygen and organic-matter gradients on the eastern Pacific Ocean, J. Mar. Res., 49, 763-800, doi: 10.1357/002224091784995756, 1991.

Liesicki L.E., Raymo, M.E.: A Pliocene-Pleistocene stack of 57 globally distributed benthic δ18O records, Paleoceanography, 20, 1, doi: 10.1029/2004PA001071, 2005.

Mallon, J.: Benthic foraminifera of the Peruvian and Ecuadorian continental margin, PhD Dissertation, Christian-Albrechts-Universität zu Kiel, 236 p., 2012.

Martin, J.H., Kanuer, G.., Karl, D.M., Broenkow, W.W.: VERTEX: carbon cycling in the northeast Pacific, Deep-Sea Res., 34, 267-286, doi: 10.1016/0198-0149(87)90086-0, 1987.

McCorkle, D.C., Keigwin, L.D., Corliss, B.H., Emerson, S.R.: The influence of microhabitats on the carbon isotopic composition of deep-sea benthic foraminifera, Paleoceanography, 5, 2, 161-185, doi: 10.1029/PA005i002p00161, 1990.

McKay, J.L., Pedersen, T.F., Kienast, S.S.: Organic carbon accumulation over the last 16 kyr off Vancouver Island, Canada: evidence for increased marine productivity during the deglacial, Quaternary Sci. Rev., 23, 261-281, doi: 10.1016/j.quascirev.2003.07.004, 2004.

McManus, J., Berelson, W.M., Severmann, S., Poulson, R.L., Hammond, D.E., Klinkhammer, G.P., Holm, C.: Molybdenum and uranium geochemistry in continental margin sediments: Paleoproxy potential, Geochim. Cosmochim. Acta, 70, 4643-4662, doi:10.1016/j.gca.2006.06.1564, 2006.

Meyer, K. M., Kump, L. R.: Oceanic euxinia in earth history: causes and consequences, Annu. Rev. Earth Pl. Sc., 36, 251–288, doi: 10.1146/annurev.earth.36.031207.124256, 2008.

Meyers, S.R., Sageman, B.B., Arthur, M.A.: Obliquity forcing of organic matter accumulation during Oceanic Anoxic Event 2, Paleoceanography, 27, doi: 10.1029/2012PA002286, 2012.

Mollier-Vogel, E., Leduc, G., Böschen, T., Martinez, P., Schneider, R.: Rainfall response to orbital and millennial in northern Peru over the last 18 ka, Quaternary Sc. Rev., 76, 29-38, doi: 10.1016/j.quascirev.2013.06.021, 2013.

Mosch, T., Sommer, S., Dengler, M., Noffke, A., Bohlen, L., Pfannkuche, O., Liebetrau, V., Wallmann, K.: Factors influencing the distribution of epibenthic megafauna across the Peruvian oxygen minimum zone, Deep-Sea Res., 168, 123-135, doi: 10.1016/j.dsr.2012.04.014, 2012.

Müller, P.J., Suess, E.: Productivity, sedimentation rate, and sedimentary organic matter in the oceans - I. Organic carbon preservation. Deep-Sea Res., 26A, 1347-1362, doi: 10.1016/0198-0149(79)90003-7, 1979.

Murray, A.W., Solomon, M.J., Kirschner, M.W.: The role of cyclin synthesis and degradation in the control of maturation promoting factor activity, Nature, 339, 280–286, doi: 10.1038/339280a0, 1989.

Owens, J.D., Gill, B.C., Jenkyns, H.C., Bates, S.M., Severmann, S., Kuypers, M.M., Woodfine, R.G., Lyons, T.W.: Sulfur isotopes track the global extent and dynamics of euxinia during Cretaceous Oceanic Anoxic Event 2. PNAS, 110, 18407-18412, doi:10.1073/pnas.1305304110, 2013.

Owens, J.D., Lyons, T.W., Li, X., Macleod, K.G., Gordon, G., Kuypers, M.M.M., Anbar, A., Kuhnt, W., Severmann, S.: Iron isotope and trace metal records of iron cycling in the proto-North Atlantic during the Cenomanian-Turonian oceanic anoxic event (OAE-2), Paleoceanography, 27, 1944-9186, doi:10.1029/2012PA002328, 2012.

Pfannkuche, O., Frank, M., Schneider, R., Stramma, L.: Climate-biogeochemistry interactions in the tropical ocean of the SE-American oxygen minimum zone Cruise No. 77, Leg 1-4 October 22 2008 – February 18, 2009 Talcahuano (Chile) – Callao (Peru) – Colon (Panama), Meteor-Berichte, 11-2, 1-200, 2011.

Pike, J., Kemp, A.E.S.: Early Holocene decadal-scale ocean variability recorded in Gulf of California laminated sediments, Paleoceanography, 12, 227-238, doi: 10.1029/96PA03132, 1997.

Poulsen, N.E., Barron, E.J., Arthur, M.A., Peterson, W.H.: Response of the mid-Cretaceous global oceanic circulation to tectonic and CO2 forcings, Paleoceanography, 16, 576-592, doi: 10.1029/2000PA000579, 2001.

Reimer, J. et al.: INTCAL13 and Marine radiocarbon age calibration curves 0-50,000 years cal BP, Radiocarbon, 55, 1869-1887, doi: 10.2458/azu_js_rc.55.16947, 2013.

Reimers, C.E., Suess, E.: Spatial and temporal patterns of organic matter accumulation on the Peru continental margin, in: Coastal Upwelling – its sedimentary record Part B: Sedimentary Records of Ancient Coastal Upwelling, edited by: Thiede, J., Suess, E., NATO Conference Series IV: Mar. Sci., Vol. 10b, 311-346, 1983.

Rein, B., Lückge, A., Reinhardt, L., Sirocko, F., Wolf, A., Dullo, W.-C.: El Niño variability off Peru during the last 20,000 years, Paleoceanography, 20, PA4003, doi: 10.1029/2004PA001099, 2005.

Rhoads, D.C., Morse, J.W.: Evolutionary and ecologic significance of oxygen-deficient basins, Lethaia, 4, 413-428, doi: 10.1111/j.1502-3931.1971.tb01864.x, 1971.

Riebesell, U.: Effects of CO_2 enrichment on marine phytoplankton, J. Oceanogr., 60, 719-729, doi: 10.1007/s10872-004-5764-z, 2004.

Rodríguez-Tovar, F.J., Uchmann, A.: Ichnological data as a useful tool for deep-sea environmental characterization: a brief overview and an application to recognition of small-scale oxygenation changes during the Cenomanian-Turonian anoxic event, Geo-Mar. Lett., 31, 525-536, doi: 10.1007/s00367-011-0237-z, 2011.

Rohling, E.J., Hilgen, F.J.: The eastern Mediterranean climate at times of sapropel formation: a review. Geol. Mijnbouw, 70, 253-264, 1991.

Sageman, B.B., Meyers, S.R., Arthur, M.A.: Orbital time scale and new C-isotope record for Cenomanian-Turonian boundary stratotype, Geology, 34, 125-128, doi:10.1130/G22074.1, 2006.

Sarnthein, M., Thiede, J., Pflaumann, U., Erlenkeuser, H., Fiitterer, D., Koopmann, B., Lange, H., Seibold, E.: Atmospheric and oceanic circulation patterns off northwest Africa during the past 25 million years, in: Geology of Northwest Africa Continental Margin, edited by: von Rad, U., Hinz, K., Sarnthein, M., and Seibold, E., Berlin- Heidelberg-New York (Springer-Verlag), 545-604, doi: 10.1007/978-3-642-68409-8_24, 1982.

Sarnthein, S., Pflaumann, U., Ross, R., Tiedemann, R., Winn, K.: Transfer functions to reconstruct ocean palaeoproductivity: a comparison, Geol. Soc. S.P., 64, 411-427, doi: 10.1144/GSL.SP.1992.064.01.27, 1992.

Savrda, C.E., Bottjer, D.J.: Trace-fossil model for reconstruction of paleo-oxygenation in bottom waters, Geology, 14, 3-6, doi: 10.1130/0091-7613, 1986.

Savrda, C.E., Bottjer, D.J.: Trace fossils as indicators of bottom-water redox conditions in ancient marine environments, Soc. Econ. PA, Pacific section, Volume and Guidebook 52, 3-26, 1987.

Savrda, C.E., Bottjer, D.J.: Oxygen-related biofacies in marine strata: an overview and update, Geol. Soc. S.P., 58, 201-219, doi: 10.1144/GSL.SP.1991.058.01.14, 1991.

Savrda, C.E., Bottjer, D.J., Gorsline, D.S.: Development of a comprehensive oxygen-deficient marine biofacies model: evidence from Santa Monica, San Pedro, and Santa Barbara Basins, California Continental Borderland, AAPG Bull. 68, 1179-1192, 1984.

Schäfer, W.: Wirkungen der Benthos-Organismen auf den jungen Schichtverband. Senck. Lethaea, 37, 183-263, 1956.

Schlanger, S.O., Jenkyns, H.C.: Cretaceous Oceanic Anoxic Events: causes and consequences, Geology, 55, 179–184, 1976.

Schnitker, D., Mayer, L.M., Norton, S.: Loss of calcareous microfossils from sediments through gypsum formation, Mar. Geol., 36, M35-M44, doi: 10.1016/0025-3227(80)90085-7, 1980.

Schönfeld, J., Schiebel, R., Timm, S.: The Rotpläner (Upper Cenomanian to Lower Turonian) of Baddeckenstedt (nort-western Germany): lithology, geochemistry, foraminifers, and stratigraphic correlations, Meyniana, 43, 73-95, doi: 10.2312/meyniana.1991.43.73, 1991.

Scholz, F., Hensen, C., Noffke, A., Rhode, A., Wallmann, K.: Early diagenesis of redox-sensitive trace metals in the Peru upwelling area – response to ENSO-related oxygen fluctuations in the water column, Geochim. Cosmochim. Acta, 22, 7247-7276, 2011.

Scholz, F., McManus, J., Mix, A.C., Hensen, C., Schneider, R.: The impact of ocean deoxygenation on iron release from continental margin sediments, Nature Geosc., 7, 433–437, doi:10.1038/ngeo2162, 2014b.

Scholz, F., Severmann, S., McManus, J., Hensen, C.: Beyond the Black Sea paradigm: The sedimentary fingerprint of an open-marine iron shuttle, Geochim. Cosmochim. Acta, 127, 368-380, doi:10.1016/j.gca.2013.11.041, 2014a

Schott, W., von Stackelberg, U., Eckhardt, F.J., Mattiat, B., Peters, J., Zobel, B.: Geologische Untersuchungen an Sedimenten des indisch-pakistanischen Kontinentalrandes (Arabisches Meer), Geol. Rundsch., 60, 246-275, 1970.

Schulz, H., von Rad, U., von Stackelberg, U.: Laminated sediments from the oxygen-minimum zone of the northeastern Arabian Sea, Geol. Soc. S.P., 116, 185-207, doi: 10.1144/GSL.SP.1996.116.01.16, 1996.

Sinninghe Damsté, J.S., Köster, J.: A euxinic southern North Atlantic Ocean during the Cenomanian/Turonian oceanic anoxic event, Earth Planet. Sc. Lett., 158, 165-173, doi: 10.1016/S0012-821X(98)00052-1, 1998.

Stein, R., Stax, R.: Late Cenozoic changes in flux rates and composition of organic carbon at Sites 798 and 799 (Sea of Japan), In: Proceedings of the Ocean Drilling Program, Scientific Results, edited by: Kenneth, A., et al., Vol.127/128, Part 1, 423-437, 1990.

Stein, R., Stax, R.: Late Quaternary organic carbon cycles and paleoproductivity in the Labrador Sea, Geo-Mar. Lett., 11, 90-95, doi: 10.1007/BF02431035, 1991.

Sterner, R., Elser, J.J.: Ecological Stoichiometry: The Biology of Elements from Molecules to the Biosphere, Princeton University Press, 2002.

Sterner, R.W., Andersen, T., Elser, J.J., Hessen, D.O., Hood, J.M., McCauley, E., Urabe, J.: Scale-dependent carbon: nitrogen: phosphorus seston stoichiometry in marine and freshwaters, American Soc. Limnol. Oceanogr., 53, 1169–1180, doi: 10.4319/lo.2008.53.3.1169, 2008.

Stramma, L., Bange, H.W., Czeschel, R., Lorenzo, A., Frank, M.: On the role of mesoscale eddies for the biological productivity and biogeochemistry in the eastern tropical Pacific Ocean off Peru, Biogeosciences, 10, 7293–7306, doi: 10.5194/bg-10-7293-2013, 2013.

Struck, U., Altenbach, A.V., Emeis, K.C., Alheit, J., Eichner, C., Schneider, R.: Changes of the upwelling rates of nitrate preserved in the δ15N-signature of sediments and fish scales from the diatomaceous mud belt of Namibia, Geobios, 35, 3-11, doi: 10.1016/S0016-6995(02)00004-9, 2002.

Stuiver, M., Reimer, P.J.: Extended C-14 data base and revised Calib 3.0 C-14 age calibration program, Radiocarbon, 35, 215-230, 1993.

Thiede, J., Suess, E. (eds.): Coastal Upwelling: Its sediment record, Part B: Sedimentary Records of Ancient Coastal Upwelling, NATO Conference Series IV: Mar. Sci., Vol. 10b, 610 p., 1983.

Thunell, R.C., Tappa, E., Anderson, D.M.: Sediment Fluxes and Varve Formation in Santa Barbara Basin, offshore California, Geology, 23, 1083-1086, doi: 10.1130/0091-7613, 1995.

Topper, R.P.M., Trabucho Alexandre, Tuenter, E., Meijer, P.Th..: A regional ocean circulation model for the mid-Cretaceous North Atlantic Basin: implications for black shale formation, Clim. Past, 7, 277–297, doi:10.5194/cp-7-277-2011, 2011.

Torrence, C., Compo, G.P.: A Practical Guide to Wavelet Analysis, Bull. Amer. Meteor. Soc., 79, 61-78, doi:10.1175/1520-0477, 1998.

Trabucho Alexandre, J., Tuenter, E., Henstra, G.A., van der Zwaan, C.J., van de Wal, R.S.W., Dijkstra, H.A. and de Boer, P.L.: The mid-Cretaceous North Atlantic nutrient trap: black shales and OAEs. Paleoceanography, 25, PA4201, doi:10.1029/2010PA001925, 2010.

Tucker, M.E.: Sedimentation of organic-rich limestones in the late Precambrian of Southern Norway, Precambrian Res., 22, 295-315, doi: 10.1016/0301-9268(83)90053-0, 1983.

van Andel, T.H.: Recent marine sediments of Gulf of California, Part 2, AAPG Special Volumes, Memoir 3, 216-310, 1964.

van Andel, T.H., Heath, G.R., Moore, T.C.: Cenozoic history and paleoceanography of the central equatorial Pacific Ocean: a regional synthesis of deep-sea drilling project data, Geol. Soc. Am. Mem., 143, 1-133, doi: 10.1130/MEM143-p1, 1975.

van Bentum, E.C., Hetzel, A., Brumsack, H.J., Forster, A., Reichart, G.J., Sinninghe Damsté, J.S.: Reconstruction of water column anoxia in the equatorial Atlantic during the Cenomanian–Turonian oceanic anoxic event using biomarker and trace metal proxies, Palaeogeogr., Palaeoclimatol., Palaeoecol., 280, 489-498, doi:10.1016/j.palaeo.2009.07.003, 2009.

van Geen, A., Zheng, Y., Bernhard, J.M., Cannariato, K.G., Carriquiry, J., Dean, W.E., Eakins, B.W., Ortiz, J.D., Pike, J.: On the preservation of laminated sediments along the western margin of North America, Paleoceanography, 18, PA1098, doi: 10.1029/2003PA000911, 2003.

Voigt, S., Schönfeld, J.: Cyclostratigraphy of the reference section for the Cretaceous white chalk of northern Germany, Lägerdorf-Kronsmoor: A late Campanian-early Maastrichtian orbital time scale, Palaeogeogr. Palaeoclimatol. Palaeocl., 287, 67-80, doi: 10.1016/j.palaeo.2010.01.017, 2010.

von Rad, U., Schulz, H. and Sonne 90 Scientific Party: Sampling the oxygen minimum zone off Pakistan: glacial-interglacial variations of anoxia and productivity (preliminary results, SONNE 90 cruise), Mar. Geol., 125, 7-19, doi: 10.1016/0025-3227(95)00051-Y, 1995.

von Stackelberg, U.: Faziesverteilung in Sedimenten des indisch-pakistanischen Kontinentalrandes (Arabisches Meer), "Meteor" Forschungs-Ergebnisse C, 9, 1-73, 1972.

Wefer, G., Dunbar, R.B., Suess, E.: Stable isotopes of foraminifers off Peru recording high fertility and changes in upwelling history, in: Coastal Upwelling – its sedimentary record Part B: Sedimentary Records of Ancient Coastal Upwelling, edited by: Thiede, J., Suess, E., NATO Conference Series IV: Mar. Sci., Vol. 10b, 295-308, 1983.

Wefer, G., Heinze, P., Suess, E.: Stratigraphy and sedimentation rates from oxygen isotope composition at the Peruvian upwelling region: Holes 680B and 686B, in: Proceedings Ocean Drilling Program, Scientific Results, edited by: Suess, E., Huene, R., et al., Vol. 112, 355-367, 1990.

Wetzel, A.: Recent bioturbation in the deep South China Sea: a uniformitarian ichnologic approach, Palaios, 23, 601-615, doi: 10.2110/palo.2007.p07-096r, 2008

Wiedmann, J., Butt, A., Einsele, G.: Vergleich von marokkanischen Kreide-Küstenaufschlüssen und Tiefseebohrungen (DSDP): Stratigraphie, Paläoenvironment und Subsidenz an einem passiven Kontinentalrand, Geol. Rundsch., 67, 454–508, doi: 10.1007/BF01802800, 1978.

Wignall, P.B., Twitchett, R.J.: Oceanic anoxia and the end Permian mass extinction, Science, 272, 1155–1158, doi: 10.1126/science.272.5265.1155, 1996.

Wolf, A.: Zeitliche Variationen im peruanischen Küstenauftrieb seit dem Letzten Glazialen Maximum – Steurung durch globale Klimadynamik, Dissertation, Christian-Albrechts-Universität zu Kiel, 115 p., 2002.

Tables

Appendix Table A1: Metadata of cores for which information about laminations were available. *: Last Glacial to 12 ka, ** chronostratigraphy based on $\delta^{18}O$ curve, *** chronostratigraphy based on correlation with cores from IODP hole 680A, -: no information available.

Cruise	Core	Latitude S	Longitude W	Depth (m)	Lamina-tions	Age model
M77/1	413	17°47.10'	72°04.44'	2166	no	-
M77/1	414	17°38.60'	71°58.38'	928	no	-
M77/1	415	17°34.39'	71°56.19'	800	no	-
M77/1	417	17°26.02'	71°51.76'	328	yes	-
M77/1	493	10°59.97'	78°44.79'	2020	no	-
M77/1	494	11°0.025'	78°44.80'	2024	no	-
M77/1	495	10°59.96'	78°34.44'	1194	no	-
M77/1	496	11°0.01'	78°34.39'	1192	no	-
M77/1	503	11°0‘	78°25.65'	699	no	-
M77/1	504	11°0.01'	78°25.67'	699	no	-
M77/1	505	11°0.01'	78°25.66'	699	no	-
M77/1	506	11°0‘	78°21.14'	521	yes	-
M77/1	507	11°0.03'	78°21.13'	520	no	-
M77/1	508	11°0.03'	78°14.19'	377	yes	-
M77/1	509	11°0.03'	78°17.18'	377	yes	-
M77/2	002-6	15°04.75`	75°44.00`	285	yes	-
M77/2	003-2	15°06.21'	75°41.28`	271	yes	yes
M77/2	005-3	12°05.66'	77°40.07`	214	yes	-
M77/2	024-5	11°05.01'	78°00.91'	210	yes	-
M77/2	026-1	10°45.13'	78°28.43'	424	yes	-
M77/2	028-3	09°17.69'	79°53:86'	1104	no	-
M77/2	029-1	09°17.70'	79°37.11'	444	yes	yes

M77/2	029-3	09°17.70'	79°37.11'	433	yes	-
M77/2	045-4	07°59.99'	80°20.51'	359	no	-
M77/2	050-4	08°01.01'	80°30.10'	1013	no	yes
M77/2	052-2	05°29.01'	81°27.00'	1249	no	yes
M77/2	053-2	05°29.02'	81°43.00'	2591	no	-
M77/2	054-1	05°29.00'	81°18.35'	299	no	-
M77/2	056-3	03°44.99'	81°07.25'	350	no	-
M77/2	056-5	03°44.99'	81°07.48'	355	no	yes
M77/2	059-1	03°57.01'	81°19.23'	997	no	yes
M77/2	060-3	03°50.98'	81°15.50'	699	no	-
M77/2	062-1	02°29.98'	81°14.72'	1675	no	-
M77/2	064-3	01°53.49'	81°11.76'	523	no	-
M77/2	065-1	01°57.01'	81°07.23'	204	no	-
M77/2	067-4	01°45.18'	82°37.50'	2080	no	-
AM77/2	069-1	03°16.00'	80°56.86'	338	no	-
M77/2	072-3	02°49.00'	81°00.53'	425	no	-
M77/2	075-1	00°13.00'	80°39.44'	1316	no	-
M77/2	076-4	00°05.45'	80°33.40'	291	no	-
W7706	40	11°15'	77°57'	186	yes	yes
W7706	41	11°20'	78°07'	411	yes	yes
W7706	44	11°24.6'	78°13.8'	580	no	yes
W7706	04	12°58'	76°57'	325	no	yes
W7706	37	13°37'	76°50'	370	yes*	yes
B0405	13	12°00.8'	77°42.64'	185	yes	yes
B0405	6	14°07.9'	76°30.1'	299	yes	yes
IODP112	680A	11°03.90'	78°04.67'	253	yes	yes**
IODP112	686A	13°28.81'	76°53.49'	447	yes	yes***
SO78	158KAL	10°57'	78°06'	237	yes	-
SO78	175KAL	11°03'	78°36'	695	no	-

SO78	173KAL-4	11°05.64'	78°01.35'	204	yes	-
SO78	162KAL-5	11°21'	78°	281	yes	-
SO78	162KAL-6	11°21'	78°	283	yes	-
SO78	172KAL	11°30'	78°09.6'	511	yes	-
SO147	34SL	9°39.55'	79°28.43'	702	no	-
SO147	46SL	9°41.43'	78°40.97'	154	yes	-
SO147	41SL	9°51.08'	79°20.31'	587	yes	-
SO147	40SL	9°51.18'	79°20.22'	597	yes	-
SO147	83SL	10°36.5'	78°44'	605	no	-
SO147	80SL	10°40'	78°51.2'	1276	no	-
SO147	97SL	11°16.5'	77°58.4'	219	yes	-
SO147	27KL	11°37'	78°02'	382	no	-
SO147	25SL	11°54.7'	78°	202	yes	-
SO147	118KA	11°56.9'	77°18'	95,8	yes	-
SO147	4SL	11°56'	77°18'	96	no	-
SO147	106KL	12°03.0'	77°39.8'	184	yes	yes
SO147	123KA	12°57.30'	77°00.10'	363	yes	-
SO147	128KA	13°30.9'	76°21'	86	yes	-
SO147	137SL	13°36.4'	76°40.6'	196	yes	-
SO147	136SL	13°36.9'	76°45.9'	282	yes	-
MW87/08	SC2	11°04.21'	-	255	yes	-
MW87/08	SC7	14°56.62'	-	105	no	-
MW87/08	SC3	15°06.16'	-	253	yes	-

1
2

Appendix Table A2. Bottom-water oxygen and organic carbon accumulation rates of Quaternary sediment cores from the Peruvian OMZ. BW: bottom water, AR: accumulation rate, *average dry bulk density for near-surface sediments at the 12°S transect off Peru, -: value not reported.

Core	Depth (m)	BW O_2 (µmol kg^{-1})	Sed. rate (cm kyr^{-1})	Dry bulk density (g/cm^3)	AR (g cm^{-2} kyr^{-1})	C_{org} (%)	C_{org} AR (g cm^{-2} kyr^{-1})	Time interval (cal ka)	Data source
W7706-40	186	2.17	-	-	28.00	13.40	3.30	0-0.5	Reimers, Suess (1983)
W7706-04	325	2.22	-	-	9.00	17.30	1.30	0-0.5	Reimers, Suess (1983)
W7706-37	370	2.65	-	-	11.00	13.20	1.60	0-0.5	Reimers, Suess (1983)
W7706-41	411	2.89	-	-	33.00	19.60	6.30	0-0.5	Reimers, Suess (1983)
SO147-106KL	184	2.10	168.8	0.36	60.38	11.25	6.79	1.5-1.9	Wolf (2002)
543MUC52	85	1.10	70	0.5*	35.00	3.50	1.23	recent	Mosch et al. (2012)
449MUC19	319	2.12	50	0.5*	25.00	10.65	2.66	recent	Mosch et al. (2012)
516MUC40	512	2.47	20	0.5*	10.00	6.07	0.61	recent	Mosch et al. (2012)
487MUC39	579	3.69	26	0.5*	13.00	6.48	0.84	recent	Mosch et al. (2012)
459MUC25	697	12.84	81	0.5*	40.50	6.72	2.72	recent	Mosch et al. (2012)
549MUC53	1005	40.34	45	0.5*	22.50	4.00	0.90	recent	Mosch et al. (2012)
M77/2-03-2	271	2.40	39.6	0.19	7.38	4.87	0.36	0.5-1.5	this study
M77/2-29-3	433	2.80	47.67	0.50	23.84	5.77	1.38	10.7-12.6	this study
M77/2-50-4	1013	53.90	23.77	0.50	11.81	3.94	0.46	11.2-14.0	this study
M77/2-52-2	1249	73.20	28.75	0.51	14.58	0.42	0.06	0-3.0	this study

Figure captions

Figure 1. Location map of the sediment cores and wells studied.

Figure 2. Oxygen concentrations of a composite section along the Peruvian continental margin and locations of sediment cores. Triangles: cores with laminated intervals. Crosses: non-laminated cores.

Figure 3. Distribution of laminated intervals in sediment cores from the Peruvian OMZ. Triangles depict age control points. All cores were radiocarbon dated except IODP 112 680 and 686, which have been dated by graphic correlation of the benthic stable oxygen isotope curve with the SPECMAP stack (Imbrie et al., 1984; Wefer et al., 1990). Note that laminations were not recorded in sediments deposited between 6 and 8 cal. ka.

Figure 4. Organic carbon accumulation rates versus bottom-water oxygen. Filled symbols indicate laminated sediment cores.

Figure 5. Onset of OAE2 in Tarfaya well SN°4. Red box indicates transition from

homogenous to laminated sediments. Note the increase in lightness variability.

Figure 6. Wavelet power spectrum of lightness values in a laminated portion of Core SN°4 (Section 41, Segment 1). Morlet wavelet with 6 parameters, the contour levels are chosen so that 75%, 50%, 25%, and 5% of the wavelet power is above each level, respectively. (Torrence and Compo, 1998).

Figure 7. Low angle truncations and small scale erosional surfaces indicating sediment reworking and re-distribution through small scale erosion and/or winnowing by bottom currents. A.-B. Coastal section near Shell/Onhym oil shale mine, lower Turonian; C. Amma Fatma coastal section, base of Turonian. Scale: 1 Dirham coin (24 mm diameter)

Figure 8. Organic carbon accumulation rates estimated from TOC measurements of 2 m continuously sampled and homogenized core sections, and density logging in Tarfaya well S13. Note the maximum between 94.4 and 93.75 Ma corresponding to the OAE-2 positive carbon isotope excursion.

1 Figure 1

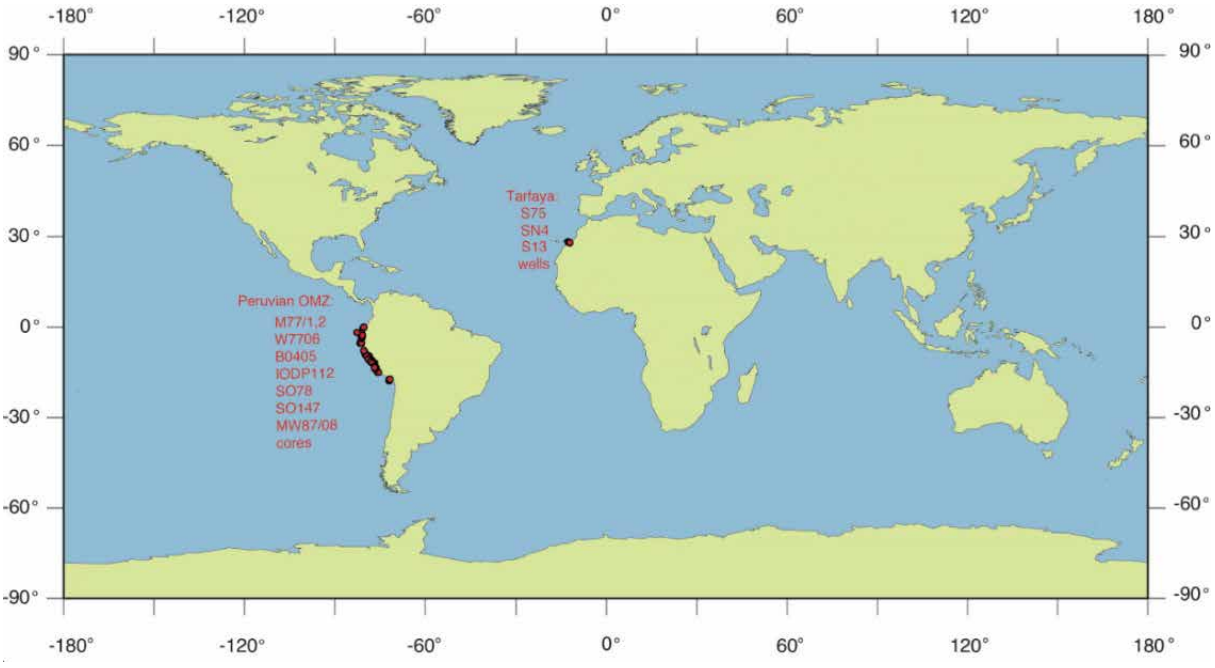

2

3 Figure 2

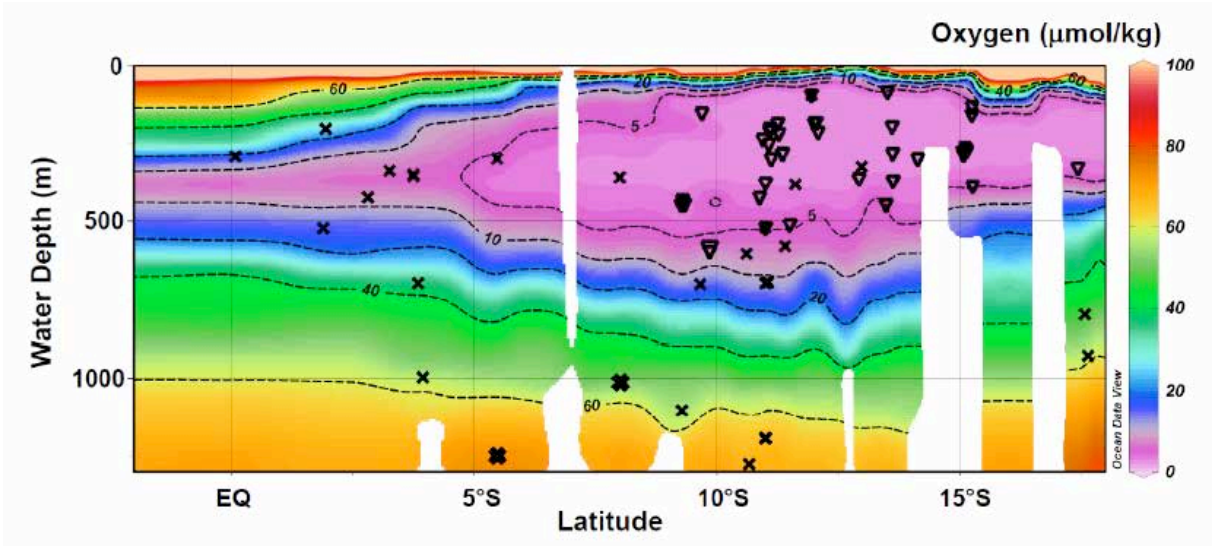

4

5

1 Figure 3

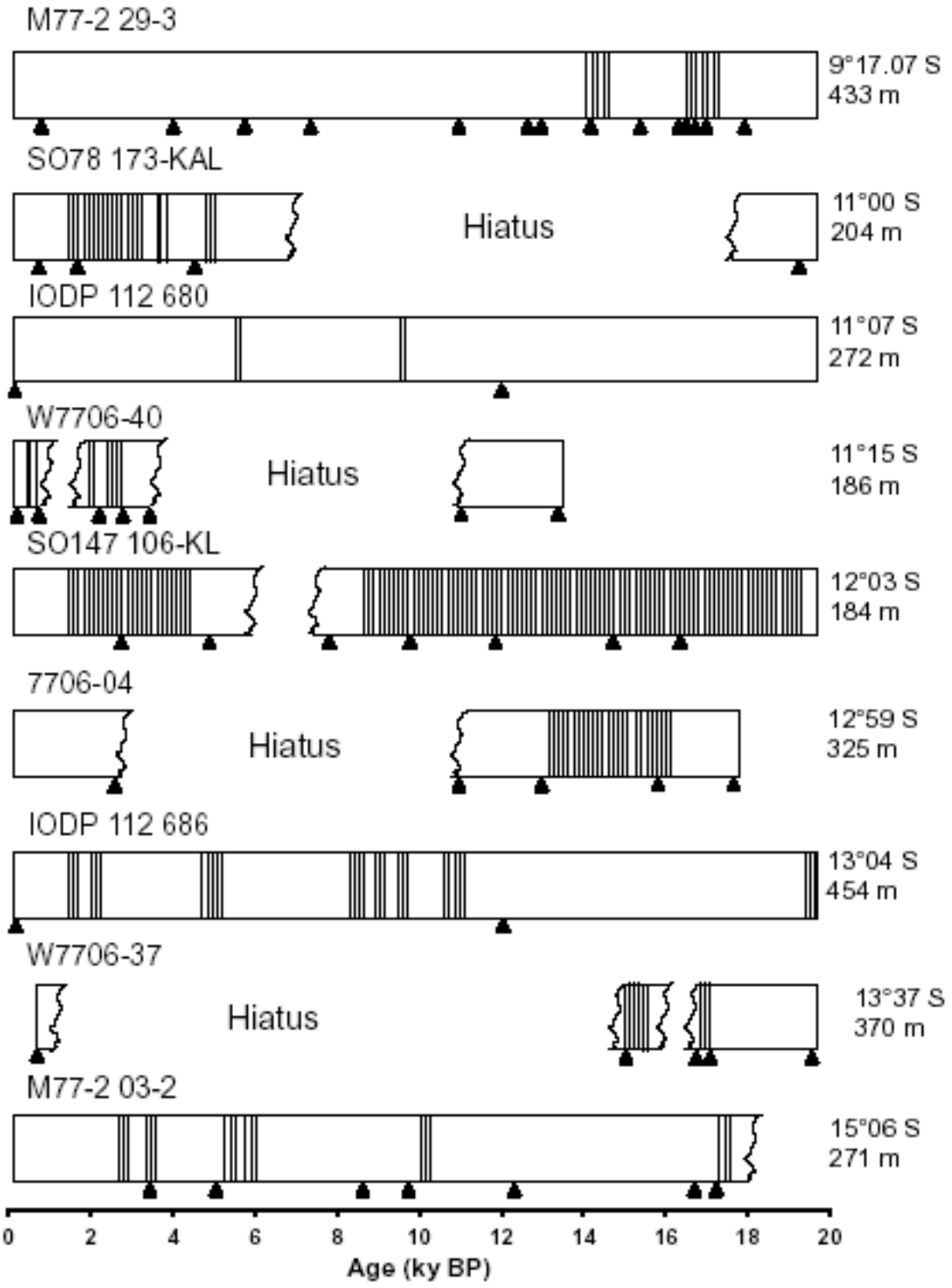
M77-2 29-3
9°17.07 S
433 m
SO78 173-KAL
Hiatus
11°00 S
204 m
IODP 112 680
11°07 S
272 m
W7706-40
Hiatus
11°15 S
186 m
SO147 106-KL
12°03 S
184 m
7706-04
Hiatus
12°59 S
325 m
IODP 112 686
13°04 S
454 m
W7706-37
Hiatus
13°37 S
370 m
M77-2 03-2
15°06 S
271 m
0
2
4
6
8
10
12
14
16
18
20
Age (ky BP)

2
3

1 Figure 4

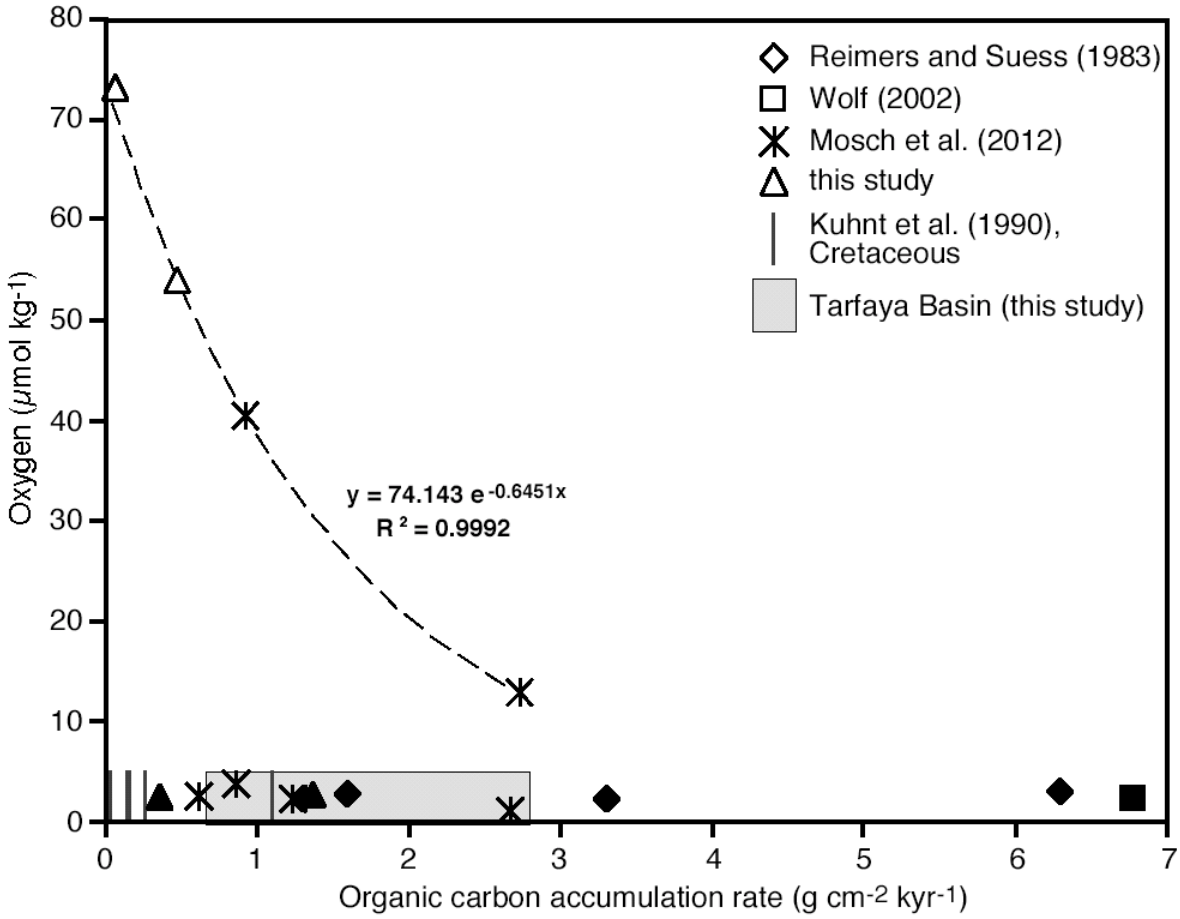

2

3 Figure 5

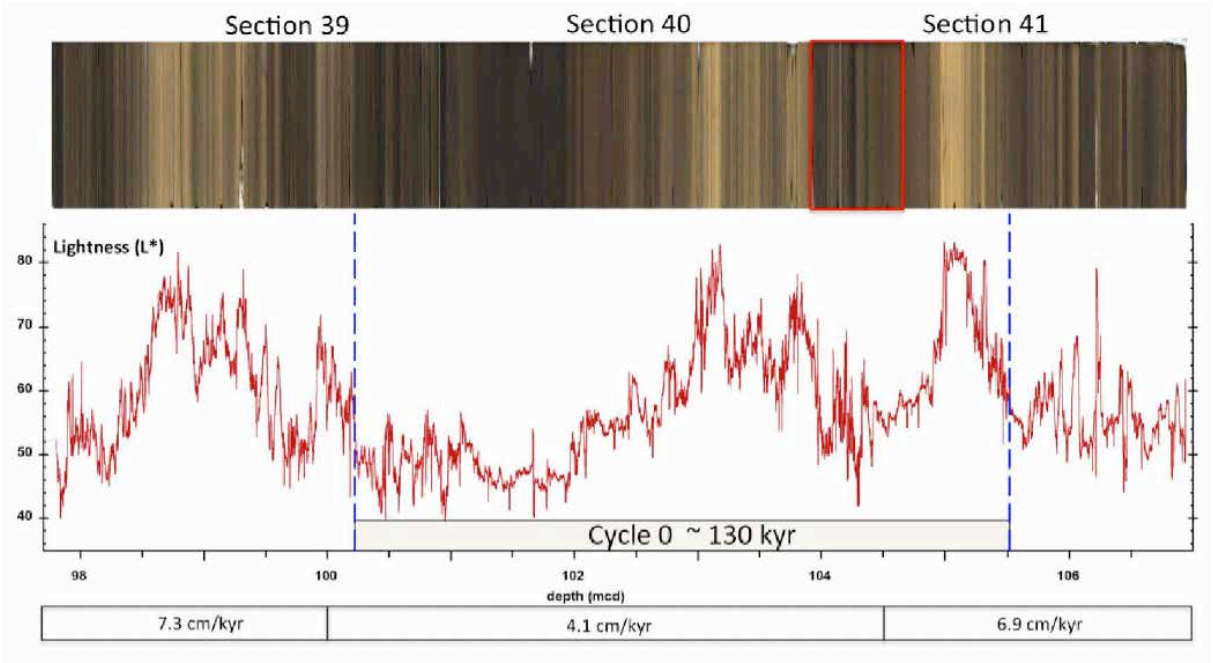

4

Figure 6

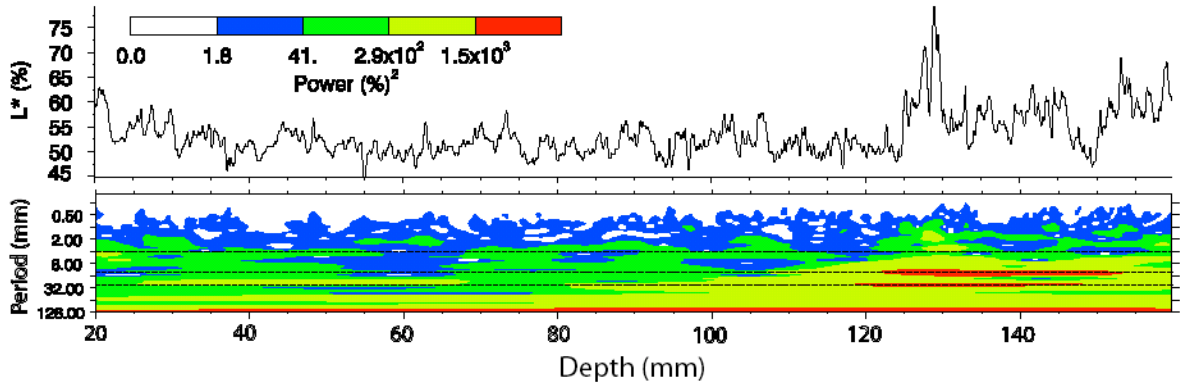

Figure 7

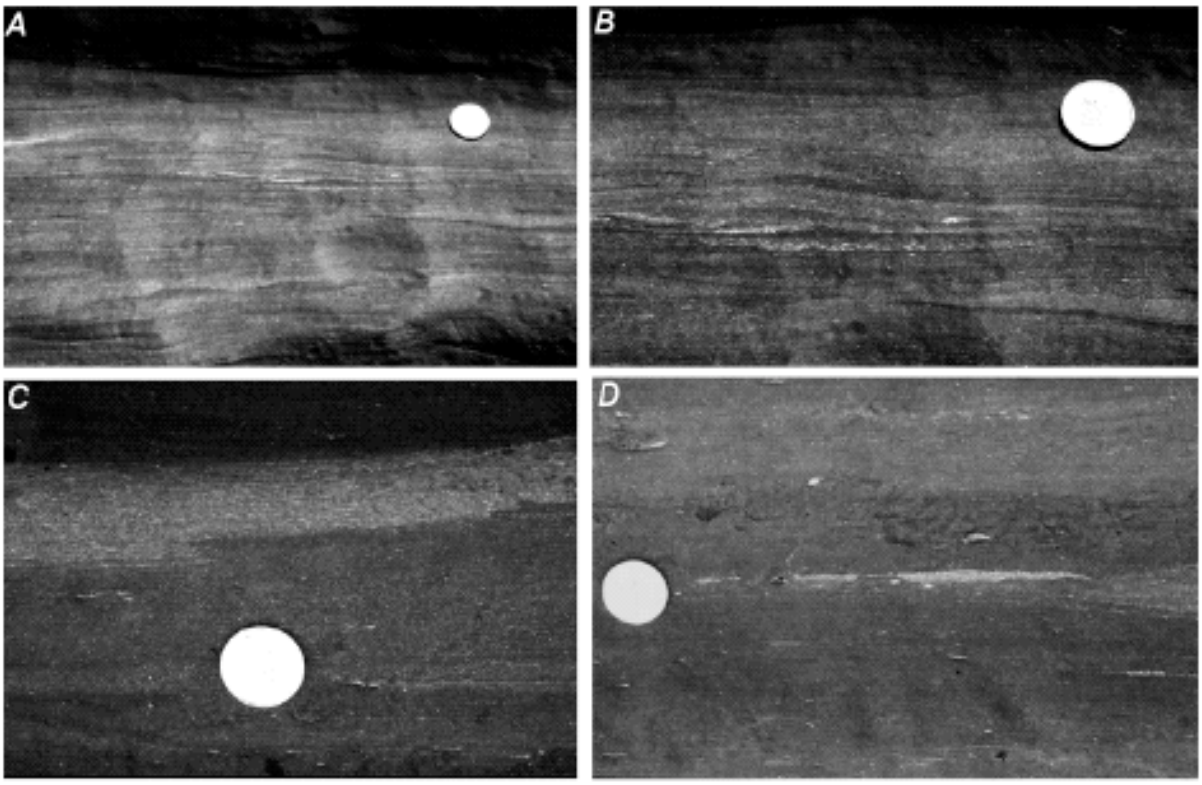

1 Figure 8

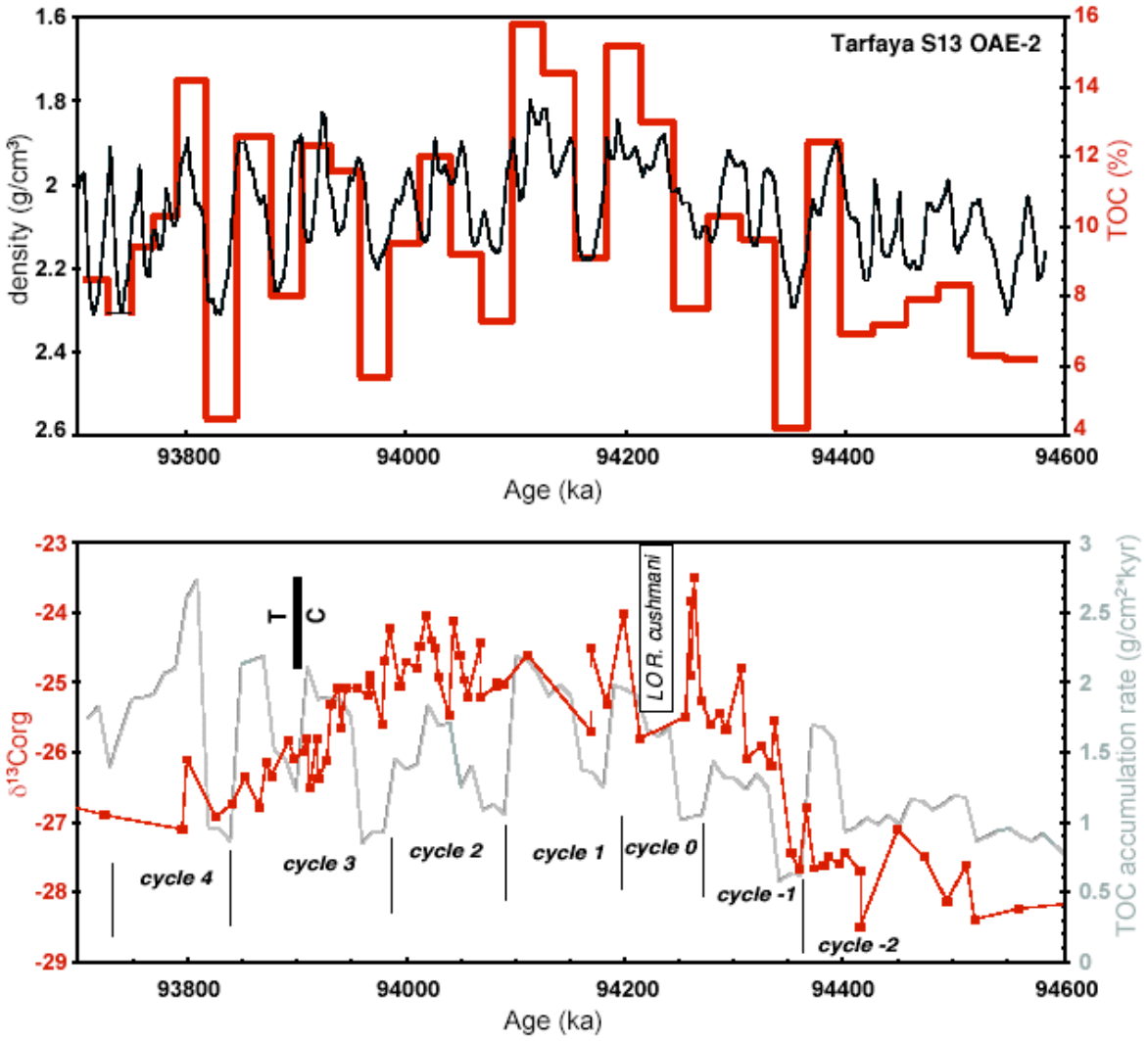
Tarfaya S13 OAE-2
density (g/cm³)
TOC (%)
Age (ka)
δ13Corg
TOC accumulation rate (g/cm²*kyr)
T
C
LO R. cushmani
cycle 4
cycle 3
cycle 2
cycle 1
cycle 0
cycle -1
cycle -2

2